FMS-300

A glossary of parameters

Document version: 1.00
Date: 19th February 2024

Hansatech
Instruments

Contents

Hansatech Instruments Ltd
Narborough Road, Pentney, King's Lynn, Norfolk PE32 1JL, UK
Tel: +44 (0)1760 338877
info@hansatech-instruments.com
www.hansatech-instruments.com

Hansatech Instruments

Hansatech Instruments Ltd
Narborough Road, Pentney, King's Lynn, Norfolk PE32 1JL, UK
Tel: +44 (0)1760 338877
info@hansatech-instruments.com
www.hansatech-instruments.com

Hansatech Instruments

1. Introduction

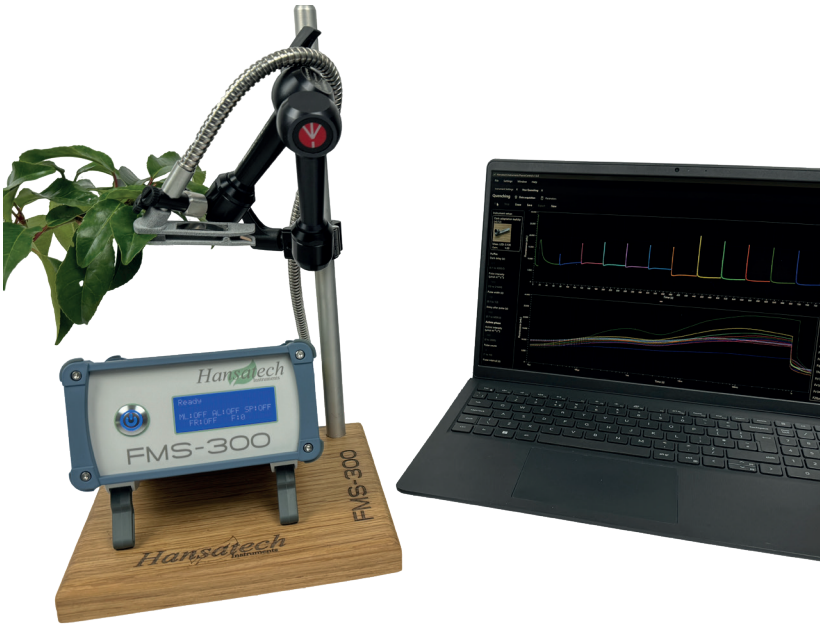

FMS-300 is a state-of-the-art, Pulse Amplitude Modulated (PAM) fluorometer combining the usability of a teaching system with the power and functionality to provide high-level research-grade data. Chlorophyll fluorescence experiments can be executed on a wide range of different samples with a comprehensive range of measured and calculated parameters presented.

Fast fluorescence data is captured, during every saturating pulse event in both light- and dark-adapted states.

Newcomers to the technique are quickly able to acquire and analyse data associated with both pulse-modulated (PAM) and fast-fluorescence (OJIP) types of fluorometry. Yet it is also a highly capable research instrument offering flexibility, functionality, and data acquisition of exceptional quality.

A wide range of features and capabilities allow the system to be used to demonstrate complex concepts, conduct experiments, collect data, analyse results, and facilitate collaborative learning or research projects.

Primarily a laboratory-based system, FMS-300 can extend to greenhouse and field applications when coupled with an appropriate portable power source.

The enviable signal quality is achieved via ultra-short measuring pulses with a standard frequency of 10 Hz (up to 100 kHz during fast fluorescence capture). At just 400 nanoseconds per pulse, FMS-300 can emit high-intensity measuring pulses with user-defined average intensities up to 0.1 µmol m-2 s-1. This combination of high intensity and ultra-short pulse width produces a strong fluorescence signal with no requirement for signal damping or data averaging. The user is presented with 100% raw instrument data.

Fast fluorescence (OJIP) kinetics are resolved during all saturating pulse events with signal-to-noise ratio comparable with that of continuous excitation fluorometers such as Handy PEA+ and Pocket PEA.

1.1 A glossary of parameters

This document provides comprehensive information of all parameters that are presented by the FMS-300. For each parameter that FMS-300 measures or calculates, this document provides:

- A definition of the parameter.
- Information on the method of calculation.
- Synonyms or logical equivalents that may be presented in the literature.
- A physiological interpretation of each parameter.
- References to publications describing the use and interpretation of the parameter.
- Graphics and theoretical background to highlight the context of parameters.

Parameters are grouped by category in the same way they are displayed in the FMS-300 FluoroControl software.

Hansatech Instruments Ltd
Narborough Road, Pentney, King's Lynn, Norfolk PE32 1JL, UK
Tel: +44 (0)1760 338877
info@hansatech-instruments.com
www.hansatech-instruments.com

Hansatech Instruments

2. Fast fluorescence & OJIP analysis

2.1 Fv/Fm: Maximum quantum yield of PSII

Maximum quantum yield of photosystem II (PSII), also known by the parameter Fv/Fm, is a fundamental measurement of chlorophyll fluorescence. Fv/Fm can be defined as the maximum quantum efficiency of PSII photochemistry (Murchie & Lawson, 2013), or, an indication of the probability that an absorbed photon will be trapped by the PSII reaction centre (RC) with the resultant reduction of Q_A (Force et al., 2003).

When a leaf is dark adapted for a sufficient period of time, the primary quinone electron acceptor of PSII, Q_A, becomes maximally oxidised and the PSII reaction centres are referred to as being "open" (Baker, 2008). In this dark-adapted state, the leaf is exposed to measuring light pulses from a fluorometer which induces a minimum level of chlorophyll fluorescence from the dark-adapted leaf. This level is termed Fo - the minimum chlorophyll fluorescence (Murchie & Lawson, 2013). Once the value for Fo is established, the dark-adapted leaf is exposed to a high-intensity saturating pulse of light for between 0.8 - 1 second which maximally reduces Q_A. At this point, the PSII reaction centres are referred to as being in a "closed" state (Baker, 2008).

In a healthy, unstressed leaf, the dark-adaptation means that there is no non-photochemical quenching (NPQ) process present (Murchie & Lawson, 2013). Therefore, there are only 2 possible fates for the light energy absorbed by the leaf during the saturating pulse:

- Photochemical quenching.
- Chlorophyll fluorescence emission.

The maximum fluorescence value recorded during the saturating pulse is therefore the maximum possible value for fluorescence and is termed Fm (Murchie & Lawson, 2013). From these 2 values Fo and Fm, Fv/Fm can be calculated thus:

$$Fv/Fm = (Fm - Fo)/Fm$$

The parameter Fv (or variable chlorophyll fluorescence) is the difference between maximum and minimum fluorescence values from a dark-adapted leaf. It demonstrates the ability of PSII to perform photochemistry (Q_A reduction) in a dark-adapted leaf (Baker, 2008).

In healthy, unstressed leaves, the Fv/Fm value is remarkably consistent. Users can expect to see values of around 0.83 which correlates to the maximum quantum yield of photosynthesis (Maxwell & Johnson, 2000 and Demmig and Björkman, 1987). Any biotic or abiotic stress factors which result in either photoinhibition or the induction of sustained quenching (Demmig-Adams and Adams, 2006), will mean that lower Fv/Fm values are measured. Therefore, the measurement of Fv/Fm following an appropriate period of dark adaptation is one of the most common techniques for measuring 'stress' in leaves (Murchie & Lawson, 2013).

2.1.1 Why measure Fv/Fm?

- **Quantum efficiency of PSII**
  Fv/Fm quantifies the proportion of absorbed photons that are efficiently used in the primary photochemistry of photosynthesis. The ability to measure Fv/Fm provides insights into the quantum mechanical aspects of energy transfer and charge separation during photosynthesis.
- **PSII damage and repair**
  Fv/Fm is an indicator of the integrity and functionality of PSII. When PSII is damaged, such as under excess light or environmental stress, Fv/Fm decreases, reflecting impaired electron transport and a reduced capacity for energy conversion. The ability to quantify this reduction is crucial for understanding the dynamics of PSII damage and repair mechanisms, which are of great interest in photosynthesis research.

- **Photoinhibition and photoprotection**
  Monitoring Fv/Fm helps in studying photoinhibition, a process where excessive light energy damages PSII. It also reveals the operation of photoprotective mechanisms, such as non-photochemical quenching (NPQ), which plants and algae employ to dissipate excess energy as heat, protecting PSII from over-excitation. Understanding the interplay between Fv/Fm and photoprotection is vital for comprehending how photosynthetic organisms adapt to changing light conditions.
- **Environmental stress physiology**
  In ecological and physiological studies, Fv/Fm serves as a sensitive marker for assessing the impact of various environmental stressors on photosynthetic performance. This includes stressors like drought, extreme temperatures, nutrient limitations, and pollutants. By quantifying Fv/Fm under different stress conditions, researchers can elucidate the underlying mechanisms of stress response and acclimation.
- **Chlorophyll fluorescence techniques**
  Advanced chlorophyll fluorescence techniques, such as fast induction (OJIP) and relaxation kinetics, can provide detailed information on energy flow within the photosynthetic apparatus. By analysing the kinetics of fluorescence, researchers can investigate not only Fv/Fm but also other parameters related to photochemical and non-photochemical quenching processes, allowing for a more comprehensive understanding of photosynthesis under dynamic conditions.
- **Mathematical modelling**
  Fv/Fm data may be used in mathematical models of photosynthesis to estimate key parameters such as the efficiency of photochemistry, the rate of electron transport, and the quantum yield of CO_2 fixation. These models are crucial for simulating and predicting the response of photosynthetic organisms to changing environmental conditions and are used in the context of climate change and ecosystem modelling.
- **Genetics and biotechnology**
  Fv/Fm measurements are integral to genetic and biotechnological research aimed at improving crop and biomass productivity. By identifying genes or mutations that enhance Fv/Fm, researchers can develop plants and algae with improved photosynthetic efficiency, which has the potential to increase food and biofuel production and mitigate the effects of climate change.

2.2 OJIP: Analysis of the fast fluorescence kinetic

OJIP analysis, or the JIP Test, can be described as a genuine signature of photosynthesis. It can be directly related to a range of different events such as redox state changes of the components involved in linear electron flow, the involvement of alternative electron routes, the build-up of transmembrane pH gradient and membrane potential, the activation of different non-photochemical quenching processes, and the activation of the Calvin-Benson cycle (Stirbet et al., 2014).

The parameters measured and calculated from this fluorescence rise provides valuable data relating to both the photochemical phase between O and J steps and the thermal phase between the J, I and P steps. Figure 1 shows a typical fast fluorescence measurement from a healthy leaf with the inflection points O, J, I and P denoted.

The fluorescence rise is plotted on a logarithmic time axis to provide greater resolution to the inflection points J and I for ease of analysis.

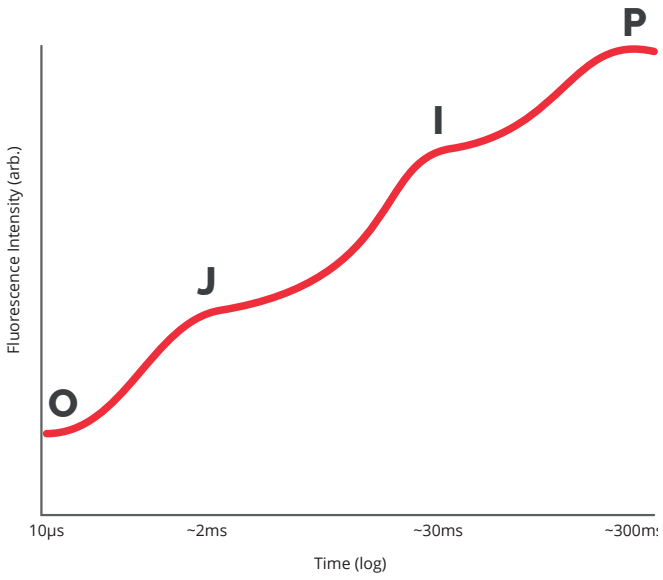

Figure 1. A typical fast fluorescence measurement from a healthy, fully dark-adapted leaf.

To assist with understanding OJIP analysis and how to relate each of the steps to physiological events, it is important to understand the photochemical events that occur in the light-dependent reactions of photosynthesis. Figure 2 below represents the Z-Scheme of photosynthesis (Hill and Bendall, 1960).

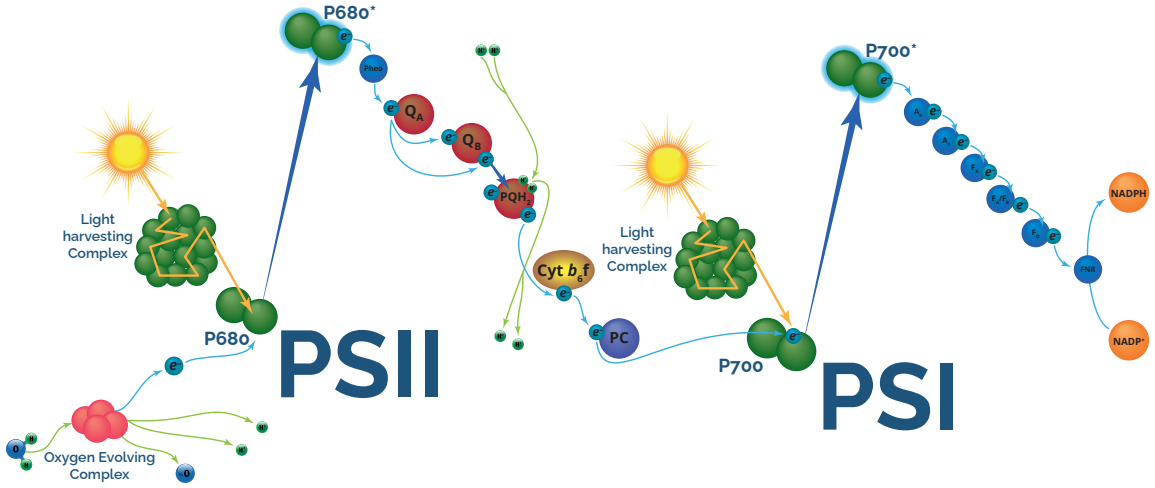

Figure 2. Graphic to show the Z-Scheme model of light-dependant reactions of photosynthesis. A more detailed and complete model of the Z-scheme by Rajni Govindjee can be seen at www.life.illinois.edu/govindjee/ZSchemeG.html

The Z-Scheme is a diagrammatic representation of the light-driven flow of electrons through the 2 photosystems ultimately reducing NADP+ to NADPH. This process also creates a proton gradient within the thylakoid lumen which is used to produce ATP from ADP and inorganic phosphate (Pi) via ATP synthase (Govindjee and Govindjee, 2000).

In a dark-adapted measurement of maximum quantum yield and OJIP, we are interested mostly in the first half of this diagram as shown in Figure 3.

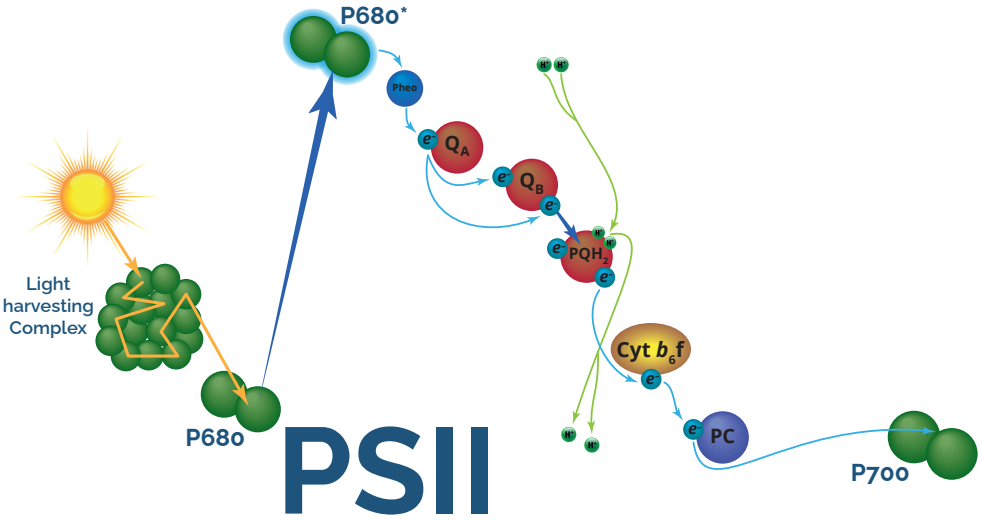

Figure 3. This graphic shows the first part of the Z-Scheme model relating to PSII photochemistry.

Fv/Fm and the OJIP analysis parameters are diagnostics for PSII photochemistry. Although PSI activity can influence electron flow though PSII, it is the reactions and electron transport of PSII that we are measuring directly. To see how a dark-adapted measurement of fast fluorescence relates to PSII activity in the light-dependent reaction, we can superimpose the graphic for PSII activity on to a typical OJIP trace from a healthy, fully dark-adapted leaf.

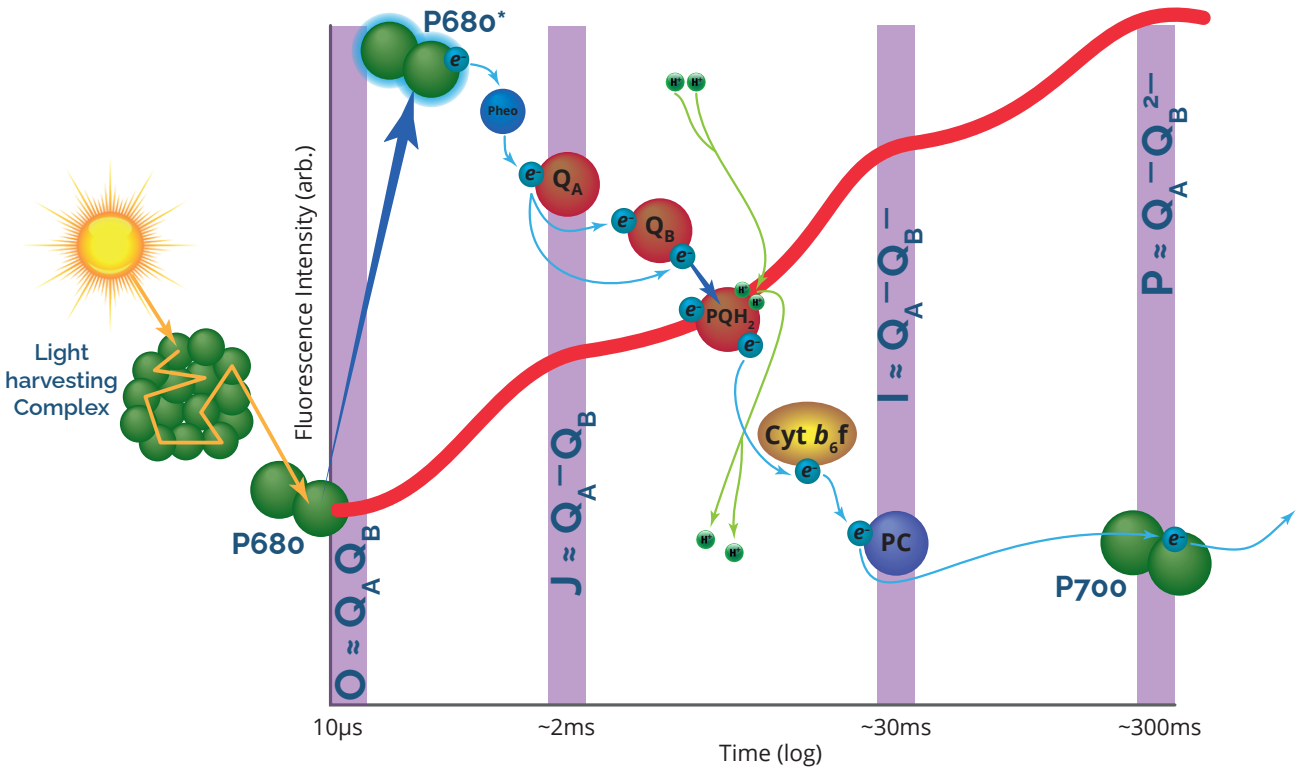

Figure 4. This graphic shows the first part of the Z-Scheme model overlaid onto a typical fast fluorescence trace. It also highlights redox states of the different elements within PSII and the electron transport chain (ETC) which links PSII to Photosystem I (PSI), shown at relevant time-points during the fast fluorescence measurement.

The fluorescence parameter Fo (or O in OJIP nomenclature) is measured under a non-actinic measuring LED only. Here, the energy states of the light harvesting complex and oxidised P680 are balanced, and the plastoquinone electron acceptors are also oxidised. Therefore, O ≈ Q_A Q_B state.

Upon illumination, P680 becomes excited to P680* and loses an electron to reduce pheophytin. Q_A is subsequently reduced to Q_A^- at the J-step, approximately 2 ms after the onset of illumination. O - J represents the photochemical phase of the fluorescence rise. The main feature of this phase is that the initial slope and relative height of the phase strongly depends on the number of photons absorbed by the sample (Stirbet & Govindjee, 2012) and therefore influenced by intensity and wavelength of the excitation/saturating light source (Lazar 2006, Strasser et al. 1995; Tomek et al. 2001).

The height of the J-step is related to the balance between reduction of Q_A and its reoxidation by Q_B . It thus reflects light-driven accumulation of Q_A^- with Q_B, the second quinone electron acceptor in PSII, being oxidised. Therefore, J ≈ Q_A^- Q_B state (Lazar 2006).

Q_B requires 2 electrons from Q_A to become fully oxidised to Q_B^{2-}, before detaching from the PSII complex and migrating into the thylakoid membrane. In addition, it collects 2 H^+ ions from the chloroplast stroma (to become PQH_2). The 2 H^+ ions are then released into the thylakoid lumen. Electrons are transferred from PQH_2 to plastocyanin (PC) via Cytochrome b_6f. Since the J-I phase reflects the light-driven accumulation of Q_B^- in addition to the accumulation of Q_A^-, I ≈ Q_A^- Q_B^- state (Lazar 2006).

The final stage of the fluorescence rise (I - P), sees electrons transferred to PSI, subsequently reducing PSI electron acceptors. The P-step at between 300 - 600 ms represents complete reduction of PSII RCs and the maximum fluorescence intensity is reached. It represents the light-driven accumulation of Q_A^- and Q_B^{2-} and therefore, Fm (or P) ≈ Q_A^- Q_B^{2-} (Lazar 2006).

The J-I-P steps of the transient are less dependent on light intensity; a greater number of photons does not result in greater fluorescence intensity (Lazar 2006, Strasser et al. 1995; Tomek et al. 2001). It was referred to as the thermal phase by Morin in 1964 after he observed that the J-I-P rise was quite sensitive to temperature, disappearing at subfreezing temperatures (Morin 1964, Neubauer and Schreiber 1987).

2.3 Fv/Fm and OJIP analysis compared

Fv/Fm and parameters derived from OJIP analysis are related but provide different types of information when assessing the photosynthetic performance and health of plants. All derived parameters could be considered important. Which parameters are useful can vary depending on the nature of the experiment and what you are hoping to study.

OJIP analysis parameters such as the Performance Index (PI, Strasser et al. 2000) is a comprehensive value that can be used as an indicator of plant vitality. PI incorporates several aspects of the OJIP transient, such as the amplitude and kinetics of the J and I steps. It quantifies the overall photosynthetic performance and stress tolerance of the plant. Other parameters describe the specific phases of the OJIP transient, allowing researchers to gain insights into the redox state of various electron transport components within the photosynthetic apparatus as shown in the table below.

Analysis	Fv/Fm	OJIP
Temporal Information	Provides a snapshot of PSII efficiency. It measures the overall performance of PSII but does not capture the dynamic changes that occur during the initial stages of photosynthesis.	Offers a time-resolved view of the photosynthetic response. It breaks down the fluorescence transient into specific phases or bands (O-J, J-I, I-P) and provides information about the kinetics of electron transport. This can help reveal subtle details about the functionality of PSII and other components of the photosynthetic machinery.
Stress Detection	Primarily used as an indicator of stress in plants. A decrease in Fv/Fm can signal that plants are under stress, but it does not provide details about the specific nature or timing of the stress response.	Can detect and quantify the impact of stress on various stages of the photosynthetic electron transport chain. By analysing changes in the OJIP transient, researchers can pinpoint which part of the photosynthetic process is affected and how the plant copes with stress. This allows for a more precise assessment of stress responses and tolerance mechanisms.
Comprehensive Assessment	A single parameter that represents the maximum photochemical efficiency of PSII. It provides a valuable but limited view of photosynthetic performance.	Involves the examination of multiple parameters, including the amplitudes and kinetics of the O, J, I, and P phases. These parameters offer a more comprehensive understanding of the entire photosynthetic electron transport chain and the functionality of different components, such as PSII, PSI, and the electron transport chain.
Diagnosis and Research	Often used for routine stress assessment and to identify unhealthy or stressed plants in agriculture and ecology.	Frequently employed in research settings to delve deeper into the underlying mechanisms of photosynthesis, stress responses, and plant physiology. It is a valuable tool for in-depth studies and investigations aimed at understanding the finer details of photosynthetic processes.

2.4 Dark-adapted samples

2.4.1 Parameters: Fast fluorescence kinetics

The following parameters should be measured on a fully dark-adapted sample.

Parameter	Synonyms	Calculation	References
Fo	DIo / CSm ABS / CSo	Calculated from an average of data points preceding a saturating pulse event	Baker (2008) Banks (2017) Srivastava et al. (1997)
Interpretation		The level of fluorescence emission when all the primary quinone acceptors (Q_A) are in the oxidized or open state. An increase in Fo has been attributed to the physical separation of the PSII reaction centres from their associated pigment antennae resulting in blocked energy transfer to PSII traps.	
Fm	P Fp ABS / CSm	Maximum average of 4 points during a saturating pulse event (see TFm)	Stirbet and Govindjee (2011) Strasser et al. (2004) Samborska et al. (2019)
Interpretation		Fluorescence intensity recorded from a dark-adapted leaf during a saturating pulse event of sufficient intensity to fully reduce all PSII reaction centres. Represents the light-driven accumulation of Q_A^- and Q_B^{2-} and therefore, Fm (or P) ≈ $Q_A^- Q_B^{2-}$ state.	
Fv	-	Fm - Fo	Baker (2008) Stirbet and Govindjee (2011) Strasser et al. (2004)
Interpretation		Demonstrates the ability of PSII to perform photochemistry (Q_A reduction) in a dark-adapted leaf.	
TFm	Tfmax	Finds the average of each group of four consecutive points over the entire range of data, finds the maximum 'average' and then saves the time for the 3rd point in that average	Strasser et al. (2004) Kalaji et al. (2017) Hassannejad et al. (2020)
Interpretation		Time to maximal fluorescence (Fm) and an indicator of Q_A reduction rate of the PSII acceptor. It is likely that this parameter has a strong sensitivity to the PSII/PSI ratio and the size of the PSI acceptor-side pool.	
Area	-	The average level between each pair of two points multiplied by the time difference between those two points, summed for all points between the start (TFo or TF1 dependent on user selection) and TFm	Rohacek and Bartak (1999) Strasser et al. (2004) Kalaji et al. (2017)
Interpretation		The area above the fluorescence induction curve measured on a dark-adapted leaf. It is proportional to the pool size of the electron acceptors Q_A on the reducing side of PSII. A useful parameter to probe electron transport capacity.	
$F_{20\mu s}$	-	-	-
Interpretation		Fluorescence value at 20µs following onset of a saturating pulse. Used as an estimation of Fo in devices that do not measure Fo using a modulated measuring light.	

Parameter	Synonyms	Calculation	References
F_L	L $F_{100\mu s}$	-	Chen et al. (2016)
Interpretation		Fluorescence intensity at T100µs (L step) which reflects the energetic connectivity of PSII units.	
F_K	K $F_{300\mu s}$	-	Chen et al. (2016) Strasser et al. (2000) Lazár (2009) Srivastava et al. (1999) Kalaji et al. (2016)
Interpretation		Fluorescence intensity at K peak at T300µs relating to the inactivation of the OEC. A well-documented symptom of heat stress, and is thought to indicate the separation of the OEC complex and electron transport between pheophytin and primary electron acceptor Q_A. The direct cause of the K peak is the outflow of electrons from P680 to PSII acceptors, which over-compensates the inflow of electrons from the donor side of PSII to P680. The K peak is also affected by changes in the energetic relationships between photosystems II. An increase in the F_K:F_J ratio indicates that the heat stress is inhibiting the donation of electrons by the OEC.	
F_J	J F_{2ms}	-	Bednarikova et al. (2020) Lazár (2006) Strasser and Govindjee (1992)
Interpretation		F_J marks the end of the O–J phase of the fluorescence induction. O–J is regarded as the photochemical phase since its height depends on intensity of used excitation light. O–J is related to the balance between reduction of Q_A and its reoxidation by Q_B. The J step therefore reflects light-driven accumulation of Q_A^- with Q_B, the second quinone electron acceptor in PSII, being oxidised. Therefore, J ≈ $Q_A^- Q_B$ state.	
F_I	I F_{30ms}	-	Lazár (2006) Strasser and Govindjee (1992)
Interpretation		F_I is the mid-point of the J-I-P thermal phase of the fluorescence induction. It is known as the thermal phase since greater light intensities do not result in greater fluorescence intensity and therefore cannot be photochemical in nature. Reflects the light-driven accumulation of Q_B^- in addition to the accumulation of Q_A^-. Therefore, I ≈ $Q_A^- Q_B^-$ state.	

Hansatech Instruments Ltd
Narborough Road, Pentney, King's Lynn, Norfolk PE32 1JL, UK
Tel: +44 (0)1760 338877
info@hansatech-instruments.com
www.hansatech-instruments.com

Hansatech Instruments

Figure 5 shows a graphical representation of where each of the parameters in the table above are taken on the fast fluorescence curve.

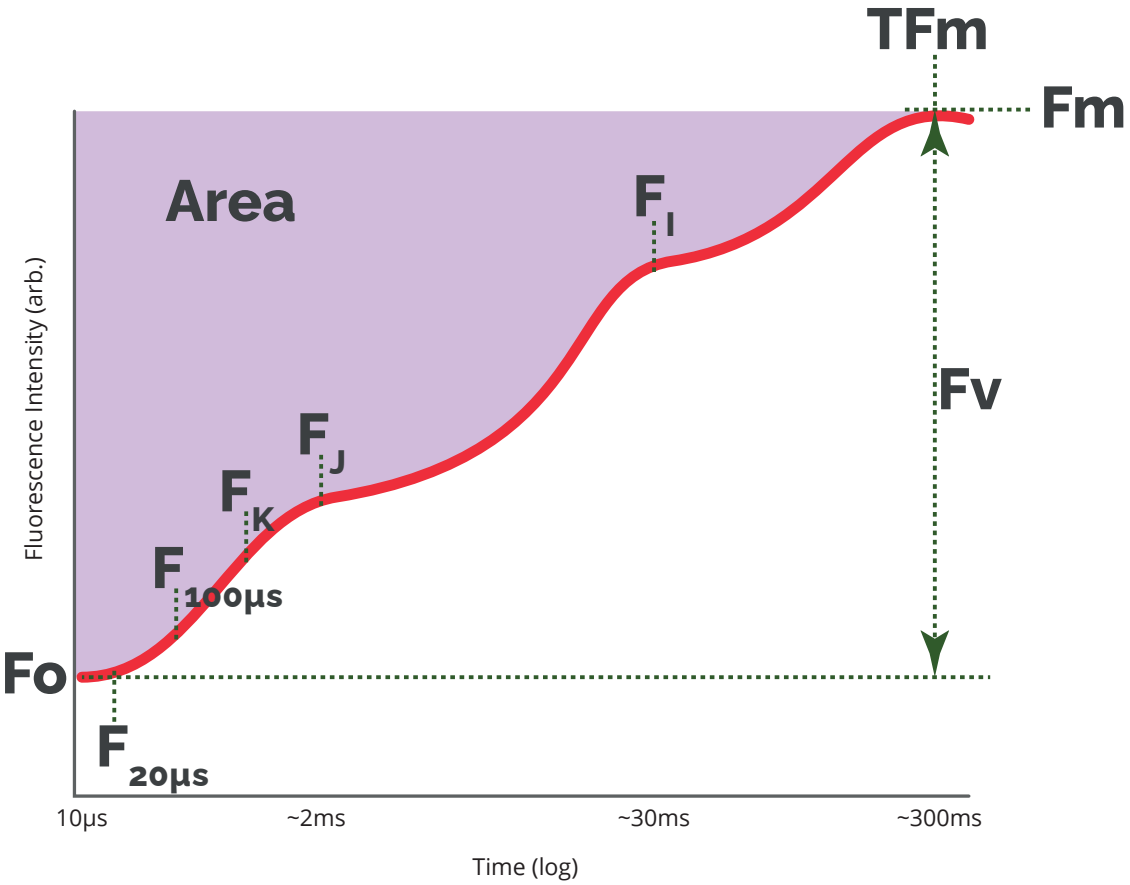

Figure 5. Annotated graph showing the points on the fast fluorescence curve where fast fluorescence kinetic parameters are measured.

2.4.2 Parameters: Fast fluorescence ratios

The following parameters should be measured on a fully dark-adapted sample.

Parameter	Synonyms	Calculation	References
Fv/Fm	φPo TRo/ABS	(Fm - Fo) / Fm	Maxwell and Johnson (2000) Rosenqvist et al. (2003) Baker (2008) Force et al. (2003) Murchie and Lawson (2013)
Interpretation		Maximum quantum efficiency of PSII. Indicates the probability that an absorbed photon will be trapped by the PSII RC with the resultant reduction of Q_A.	
Fv/Fo	-	(Fm - Fo) / Fo	LI Rong-hua et al. (2006) Stirbet and Govindjee (2011) Strasser et al. (2004)
Interpretation		Estimates the maximum primary yield of photochemistry of PSII to provide an estimation of leaf photosynthetic capacity. It is also related to maximal efficiency of the water splitting reaction (also oxygen evolution) on the donor side of PSII.	

Parameter	Synonyms	Calculation	References
Fo/Fm	-	Fo/Fm	Banks (2017) Gliožeris et al. (2007)
Interpretation		Ratio of extrema. An indicator of the physiological state of the photosynthetic apparatus.	
V_J	-	$(F_J - Fo) / (Fm - Fo)$	Dewez et al. (2018) van Rensburg et al. (1996)
Interpretation		Represents the relative emission of variable Chl a fluorescence at 2 ms (the J-step). Estimates the fraction of PSII Q_A acceptors in the reduced state ($Q_A^-/Q_{A(total)}$)	
V_I	-	$(F_I - Fo) / (Fm - Fo)$	Strasser et al. (2004) Kalaji et al. (2017)
Interpretation		Relative variable fluorescence at 30 ms the (I-step). This expression has no direct reference to changes in PSII	

Figure 6 shows a graphical representation of how each of the parameters in the table above are calculated from the fast fluorescence curve.

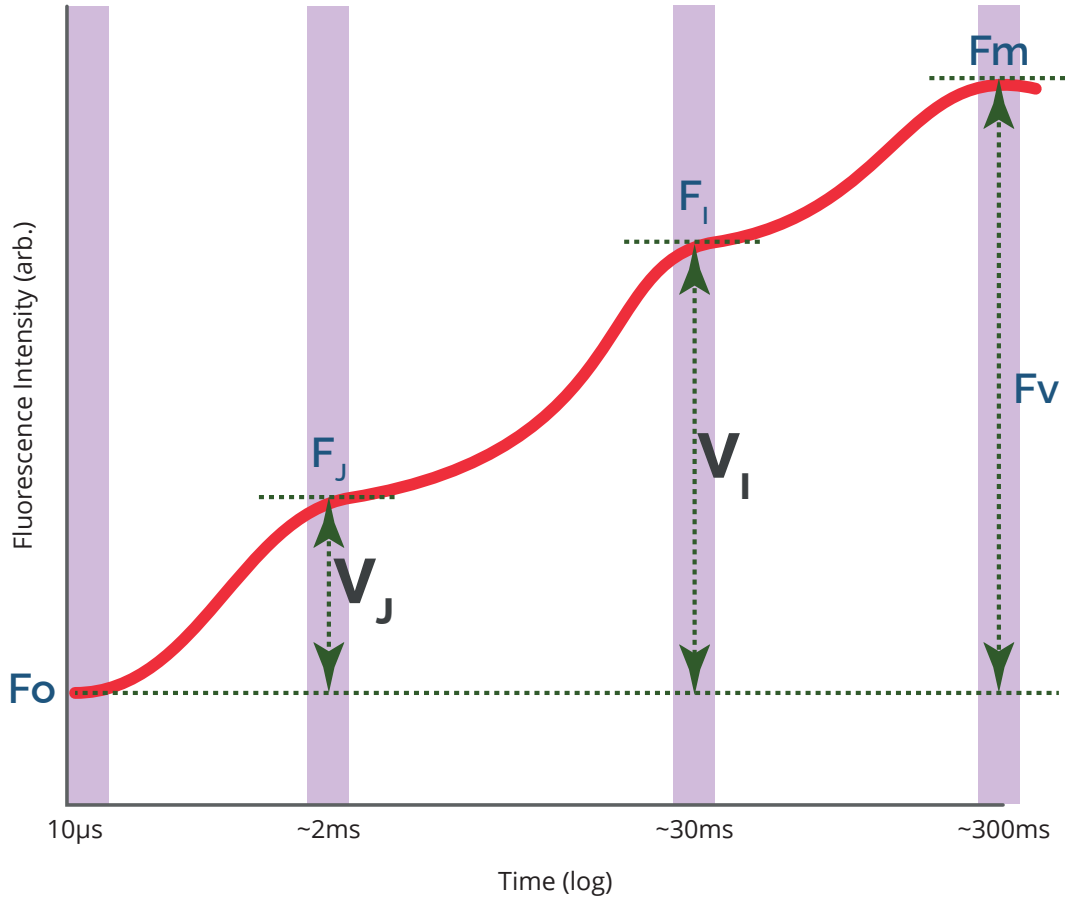

Figure 6. Annotated graph showing the how the ratio parameters are calculated from the fast fluorescence curve.

Hansatech Instruments Ltd
Narborough Road, Pentney, King's Lynn, Norfolk PE32 1JL, UK
Tel: +44 (0)1760 338877
info@hansatech-instruments.com
www.hansatech-instruments.com

2.4.3 Parameters: Slopes & integrals

The following parameters should be measured on a fully dark-adapted sample.

Parameter	Synonyms	Calculation	References
RC/ABS	γ(RC) / ((1 - γ(RC))	(V_J / Mo) x (Fv / Fm)	Barboričová et al. (2022)
Interpretation		The ratio of the total number of reaction centres to the total number of photons absorbed by the chlorophyll molecules of all reaction centres. Expresses the average size of the active reaction centre (RC) antennas.	
dVg/dto	(ΔVg/Δt)o	(1ms / (TF_L - TFo)) x ((F_L – $F_{20\mu s}$) / (Fm - Fo))	Strasser et al. (2004) Stirbet & Govindjee (2011)
Interpretation		Expresses the excitation energy transfer between the reaction centres.	
N	-	Sm x Mo x (1 / V_J)	Force et al. (2003) Tsimilli-Michael (2020)
Interpretation		Time-dependent turnover number of Q_A. Expresses how many times Q_A has been reduced in the time interval between TFo to TFm.	
Sm	-	Area / Fv	Tsimilli-Michael (2020) Stirbet & Govindjee (2011)
Interpretation		Normalization of the Area parameter on the maximum variable fluorescence, necessary to compare samples under different conditions. Provides a measure of the excitation energy needed to be supplied (by open units) in order to close all RCs. It thus expresses a work integral and also provides a measure of the amount (on an arbitrary scale) of all electron carriers reduced from TFo until TFm. It is assumed proportional to the number of reduction and oxidation of one Q_A^- molecule during the fast OJIP transient, and therefore related to the number of electron carriers per ETC.	
Sm/TFm	-	Sm / ((TFm) x 1000)	Strasser et al. (2004)
Interpretation		The average redox state of Q_A in the time span from 0 to TFm, namely the average fraction of open reaction centres during the time needed to complete their closure. Provides a measure of the average electron transport activity.	
Mo	(ΔV/Δt)o dV/dto	(1ms / (TF_K - TFo)) x ((F_K - Fo) / (Fm - Fo)) or (0.001 / (0.0003 - 0)) x (F_K - Fo) / (Fm - Fo)	Force et al. (2003) Tsimilli-Michael (2020)
Interpretation		Net rate of PSII closure in ms^{-1}. An approximation of the slope at the origin of the fluorescence rise (ΔV/Δt)o. A measure of the rate of primary photochemistry. A net rate because reduced Q_A can be reoxidised via electron transport beyond Q_A. In many publications, Mo is calculated using the F50µs point for Fo. F50µs is regarded as a "reliable" first data point in non-PAM fluorometers typically used for measurement of Mo. PAM-type fluorometers measure dark-adapted Fo under the measuring LED only where all PSII RCs are oxidised. The Fo is therefore accurate and can be used in the calculation of Mo. Figure 7 illustrates how the value of Mo can be affected depending on which value is used for Fo in the parameter calculation.	

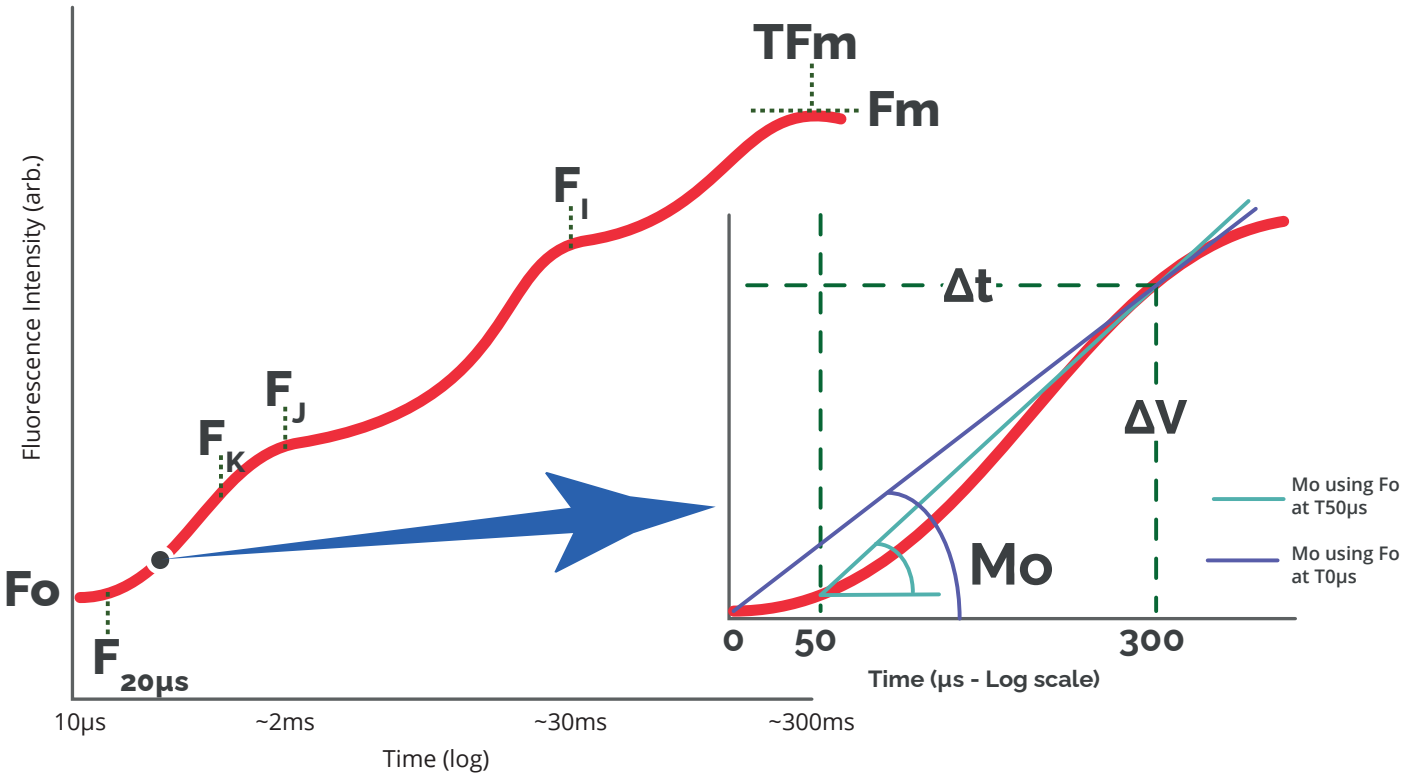

Figure 7. Graph to show how using a true Fo in a PAM-type fluorometer compared with the fluorescence value at 50µs (typically associated with non-modulated fluorometers) affects the calculation of the Mo parameter.

2.4.4 Parameters: Yield:flux ratios

The following parameters should be measured on a fully dark-adapted sample.

Parameter	Synonyms	Calculation	References
φPo	TRo / ABS Fv / Fm	1 - Fo / Fm	Force et al. (2003)
Interpretation		Trapping efficiency/probability (Fv/Fm ratio). The efficiency/probability that an absorbed photon will be trapped by the PSII RC with the resultant reduction of Q_A. Relates to the whole measured sample that may be heterogeneous in terms of Q_A reducing and non-reducing RCs.	
φEo	ETo / ABS Φ_{ET2o}	1 - F_J / Fm	Tsimilli-Michael (2020) Gonzalez-Mendoza et al. (2006) Küpper et al. (2019)
Interpretation		The quantum yield for electron transport. Expresses the probability that an absorbed photon will move an electron into electron transport further than Q_A^-	
φRo	REo / ABS	$(1 - V_I) / (1 - V_J)$	Cuchiara et al. (2013)
Interpretation		The quantum yield for the reduction of the final PSI electron acceptor per photon absorbed.	

Parameter	Synonyms	Calculation	References
ψEo	ETo / Tro ψ_{ET20}	$1 - V_J$	Force et al. (2003) Tsimilli-Michael (2020) Gonzalez-Mendoza et al. (2006) Küpper et al. (2019)
Interpretation		Electron transport efficiency/probability. The efficiency/probability that a trapped exciton, having triggered the reduction of Q_A to Q_A^-, can move an electron further than Q_A^- into the electron transport chain.	
δRo	REo / Eto Φ_{RE10}	$1 - F_I / Fm$	Cuchiara et al. (2013) Küpper et al. (2019)
Interpretation		The efficiency/probability that an electron of the intersystem electron carriers moves to reduce the final PSI electron acceptors (the likelihood of the reduction of a final PSI acceptor).	

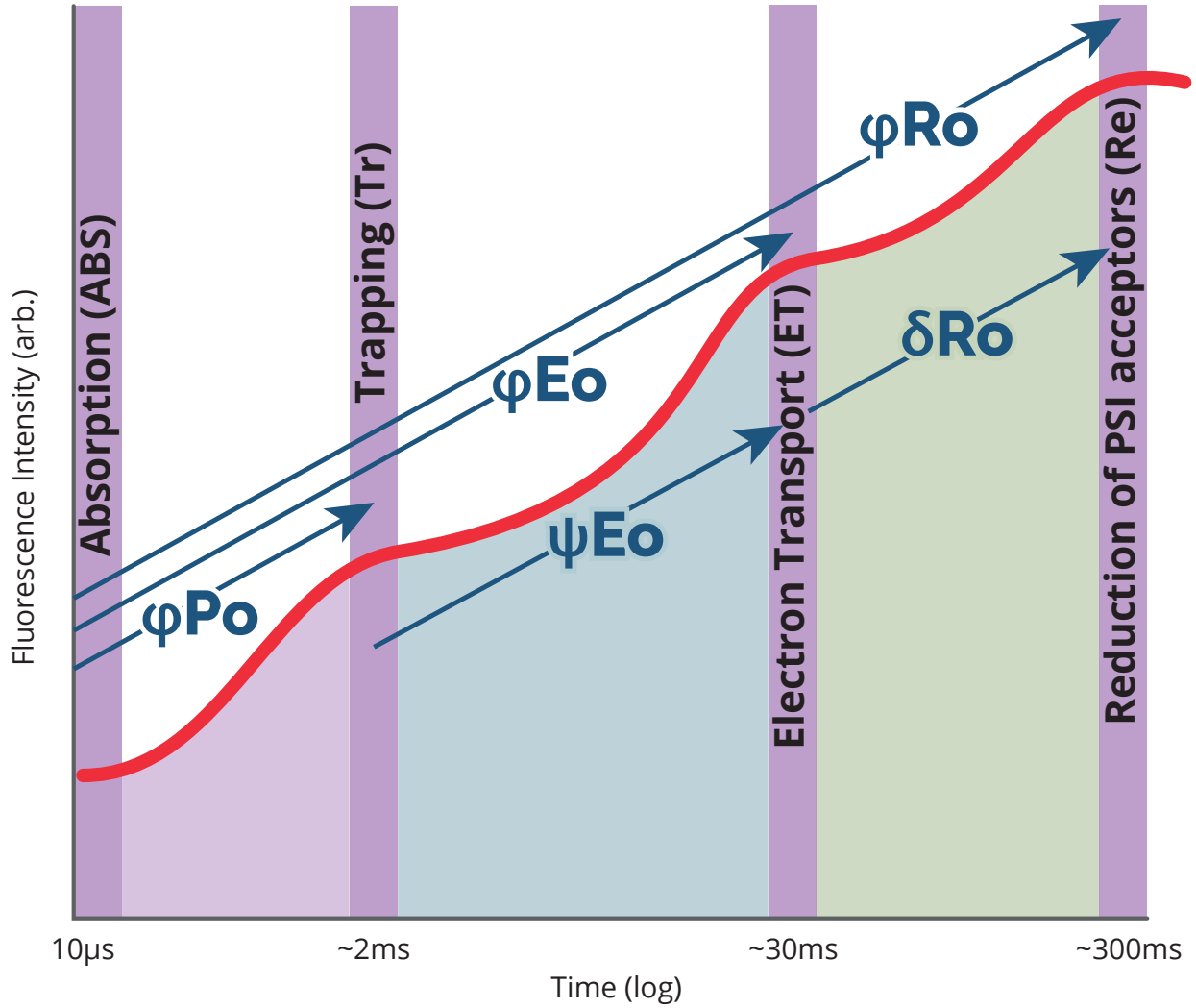

Figure 8. Graph to show context for the yield:flux ratio parameters. The arrows indicate which part of the OJIP kinetic each of the parameter values represents.

2.4.5 Parameters: Performance indices and driving forces

The following parameters should be measured on a fully dark-adapted sample. An interpretation of the parameters shown is given below the table.

Parameter	Calculation	References
PI_{abs}	(γRC / 1-γRC) x (φPo / 1-φPo) x (ψEo / 1-ψEo) or (RC / ABS) x (Fv / Fo) x ((1 - V_J) / V_J)	Tsimilli-Michael (2020) Strasser et al. (2000) Strasser et al. (2004) Tsimilli-Michael & Strasser (2008)
PI_{total}	(γRC / 1-γRC) x (φPo / 1-φPo) x (ψEo / 1-ψEo) x (δRo / 1 - δRo) or (RC / ABS) x (Fv / Fo) x ((1 - V_J) / V_J) x ((1 - V_I) / (V_I - V_J))	
DF_{abs}	$Log(Pi_{abs})$	
DF_{total}	$Log(PI_{total})$	

Interpretation

The performance index PI_{abs} was introduced as a product of terms expressing energy bifurcations from the absorption events to the reduction of the intersystem electron transport chain. When extended as PI_{total}, the index also incorporates the energy bifurcation until the reduction of PSI end electron acceptors. As defined, the performance indexes are products of unit-less [pi/(1 − pi)] terms, where pi (i = 1, 2, ..., n) stands for probability (or fraction); hence, the terms express partial performances.

Such expressions are related to the Nernst equation, where pi is the fraction of the reduced and (1 - pi) the fraction of the oxidised form of a compound; in that case log[pi/(1 − pi)] expresses the potential or driving force for the corresponding oxidoreduction reaction. Extrapolating this inference from chemistry, the $log(PI_{abs})$ was defined as the total driving forces DF_{abs}, which is the sum of partial driving forces. Since the calculated values of PI_{abs} and PI_{total} are on an arbitrary scale, they cannot be used to characterise a sample. It is how they change within samples of the same photosynthetic material, whatever the cause, that is meaningful. Hence the $[PI_{total}]/[PI_{total,control}]$ is mostly used and, accordingly, the $\Delta[DF_{total}] = [DF_{total}] - [DF_{total,control}]$.

The performance indexes, being very sensitive parameters (especially PI_{total}), have proven to be very useful for routine screening of plants and evaluation of the overall impact of a stress on photosynthetic performance/ behaviour. Their individual terms provide information for the impact on the sequential processes.

It is worth clarifying the following:

- Though both PI_{abs} and PI_{total} are determined from the kinetics of PSII fluorescence, PI_{total} evaluates impacts also on PSI behaviour (via the δRo term).
- When introduced, PI_{abs} was denoted as 'performance index on absorption basis', hence the subscript 'abs'. When the extended PI_{total} was defined, though, it is also on absorption basis, it had to be distinguished; hence, subscript 'total' was used.
- Like electrochemical potentials, driving forces DF_{abs} and DF_{total}, as well as any partial DF, can be positive, negative or zero, since they are the logarithms of quantities that can be bigger, smaller or equal to unity.

Tsimilli-Michael M.
Revisiting JIP-test: An educative review on concepts, assumptions, approximations, definitions and terminology.
Photosynthetica. 2020 Jan 1;58(special issue):275-92.

2.4.6 Parameters: Specific fluxes

The following parameters should be measured on a fully dark-adapted sample.

Parameter	Synonyms	Calculation	References
ABS/RC	Antenna size AZ	(Mo) x (1 / V_J) x (1 / φPo)	Force et al. (2003) Tsimilli-Michael (2020)
Interpretation		Effective antenna size of an active RC. The total number of photons absorbed by chlorophyll molecules of all RCs divided by the total number of active RCs. It is influenced by the ratio of active/ inactive RCs.	
TRo/RC	-	Mo x (1 / V_J)	Force et al. (2003) Tsimilli-Michael (2020)
Interpretation		Maximal trapping rate or trapped energy flux (leading to a Q_A reduction) of an RC. The maximal rate by which an exciton is trapped by the RC resulting in the reduction of Q_A. A situation synonymous with measuring the trapping rate in the presence of DCMU.	
ETo/RC	-	Mo x (1 / V_J) x (1 - V_J)	Force et al. (2003) Tsimilli-Michael (2020)
Interpretation		Electron transport flux (further than Q_A^-) in an active RC. The reoxidation of reduced Q_A via electron transport in an active RC. Only reflects the activity of active RCs.	
REo/RC	-	Mo x (1 / V_J) x (1 - V_I)	Tsimilli-Michael (2020)
Interpretation		Electron flux reducing end electron acceptors at the PSI acceptor side, per active RC.	
DIo/RC	-	(ABS / RC) - (TRo / RC)	Force et al. (2003)
Interpretation		Effective dissipation of an active RC. The ratio of the total dissipation of untrapped excitation energy from all RCs with respect to the number of active RCs. Dissipation occurs as heat, fluorescence and energy transfer to other systems. It is influenced by the ratio of active/inactive RCs.	

2.4.7 Parameters: Apparent fluxes (approximated by Fo)

The following parameters should be measured on a fully dark-adapted sample.

Parameter	Synonyms	Calculation	References
ABS/CSo	Fo	Fo	Force et al. (2003)
Interpretation		Number of photons absorbed by an excited PSII cross-section – the total number of photons absorbed by the antenna molecules of active and inactive PSII RCs over the sample cross-section. Represented by the dark-adapted Fo value.	
TRo/CSo	-	Fo x (1 - Fo / Fm)	Force et al. (2003)
Interpretation		Maximal trapping rate in a PSII cross-section – the maximal trapping rate of an exciton that will lead to Q_A reduction measured over a cross-section of active and inactive RCs.	

Parameter	Synonyms	Calculation	References
ETo/CSo	-	Fo x (1 - F_J / Fm)	Force et al. (2003)
Interpretation		Electron transport in a PSII cross-section – the reoxidation of reduced Q_A via electron transport over a cross-section of active and inactive RCs.	
REo/CSo	-	Fo x (1 - F_I / Fm)	Stirbet and Govindjee (2011) Strasser et al. (2004) Samborska et al. (2019)
Interpretation		Electron flux reducing end electron acceptors at the PSI acceptor side, per cross section.	
DIo/CSo	-	Fo x (Fo / Fm)	Force et al. (2003)
Interpretation		Dissipation in a PSII cross-section - total dissipation measured over the cross-section of the sample that contains active and inactive RCs. Dissipation occurs as heat, fluorescence and energy transfer to other systems.	

2.4.8 Parameters: Apparent fluxes (approximated by Fm)

The following parameters should be measured on a fully dark-adapted sample.

Parameter	Synonyms	Calculation	References
ABS/CSm	-	Fm	Strasser et al. (2004)
Interpretation		Absorption flux per cross section.	
TRo/CSm	-	Fv	
Interpretation		Trapped energy flux per cross section (at t = 0).	
ETo/CSm	-	Fm x (1 - F_J / Fm)	
Interpretation		Electron transport flux per cross section (at t = 0).	
REo/CSm	-	Fm x (1 - F_I / Fm)	
Interpretation		Electron flux reducing end electron acceptors at the PSI acceptor side, per cross section.	
DIo/CSm	-	Fo	
Interpretation		Dissipated energy flux per cross section (at t = 0).	

Modelling specific and Apparent Energy Flux parameters

Adapted from Tsimilli-Michael & Strasser (2008) [1].

The pipeline model was first proposed by Prof. Reto Strasser in 1987 [2] as a method of graphically representing specific and apparent (phenomenological) energy fluxes of the photosynthetic apparatus. The model was subsequently included as a key analysis tool within a piece of software called Biolyzer, which was originally authored and distributed by Prof. Strasser's Bioenergetics Laboratory at the University of Geneva.

The graphics in Figure 9 are stylised representations of the pipeline model and demonstrate the concept of comparing control (A) and stressed (B) samples. They are not based on specific data sets.

The 2 graphics on the left show membrane models for specific energy fluxes per reaction centre (RC). The 2 graphics on the right show leaf models for apparent energy fluxes per excited cross section (CS).

In both model types, parameters for absorption (ABS), trapping (TR), electron transport (ET) and dissipation (DI) are represented by arrows. The overall width of the arrows is dictated by the value of the respective parameter.

In the membrane model, ABS and TR by inactive RCs are indicated by the hatched lateral sections of the arrows. The proportion of antenna belonging to PSII units with inactive centres is indicated by the darker outer ellipse.

In the leaf model, open circles indicate the active RCs and closed circles the inactive centres. The darkness of the foliage indicates, qualitatively, the chlorophyll concentration per leaf cross section.

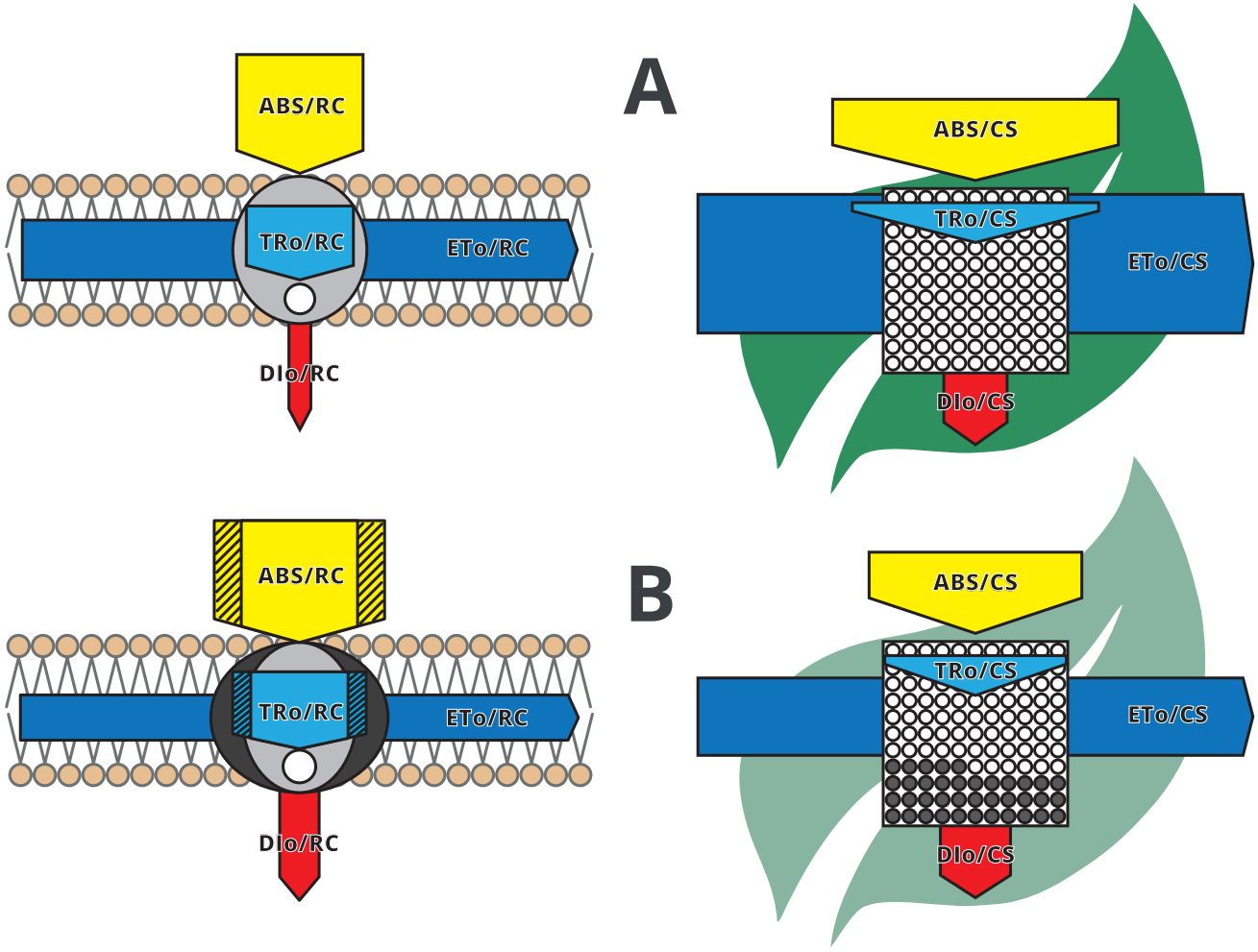

Figure 9. How the graphical Pipeline Model can be used to present specific and apparent flux parameter values.

Tsimilli-Michael, Merope & Strasser, Reto. (2008). In vivo Assessment of Stress Impact on Plant's Vitality: Applications in Detecting and Evaluating the Beneficial Role of Mycorrhization on Host Plants. 10.1007/978-3-540-78826-3_32.

Strasser, R. J. 1987. Energy pipeline model of the photosynthetic apparatus. – In Progress in Photosynthesis Research Vol. 2 (J. Biggins, ed) pp. 717–720. Martinus Nijhoff Publishers, Dordrecht . ISBN 90-247-3449-5.

Biolyzer software versions > V3.0.6 distributed by Fluoromatics (www.fluoromatics.com).

2.4.9 Parameters: De-excitation rate constants of PSII antenna

The following parameters should be measured on a fully dark-adapted sample.

Parameter	Synonyms	Calculation	References
kN	-	kN = (ABS) x kF x (1 / Fm)	Tsimilli-Michael (2020)
Interpretation		Non-photochemical de-excitation rate constant.	
kP	-	kP = (ABS) x kF x ((1 / Fo) - (1 / Fm)) or kN x (Fv / Fo)	
Interpretation		Photochemical de-excitation rate constant.	

2.5 Light-adapted samples

2.5.1 Parameters: Fast fluorescence kinetics

The following parameters should be measured on a light-adapted sample.

Parameter	Synonyms	Calculation	References
F	F', Fs', Fs, Ft', Ft	Steady state fluorescence value from light-adapted leaf.	Baker (2008) Maxwell and Johnson (2000)
Interpretation		Provides little information on photosynthetic performance because these parameters are influenced by many factors.	
Fm'	-	Maximum average of 4 points during a saturating pulse event.	Stirbet and Govindjee (2011) Strasser et al. (2004) Samborska et al. (2019)
Interpretation		Maximal fluorescence recorded under saturating illumination at when all PSII RCs are closed on a light-adapted sample.	
Fq'	ΔF	Fm' - F	Baker (2008)
Interpretation		Photochemical quenching of fluorescence by open PSII reaction centres.	
TFm'	-	Finds the average of each group of four consecutive points over the entire range of data, finds the maximum 'average' and then saves the time for the 3rd point in that average	-
Interpretation		Time to maximal fluorescence (Fm') in a light-adapted sample. Relates to the speed of complete PSII reduction in light-adapted leaves. Does not appear to have been discussed in the literature to date.	
Fo'(m)		Measurement of Fo' under far-red illumination.	Baker (2008) Maxwell and Johnson (2000)
Interpretation		By transiently shading the sample and illuminating with far-red light, PSI is preferentially excited relative to PSII allowing Q_A to rapidly become fully oxidised.	

Parameter	Synonyms	Calculation	References
Fo'(c)	-	Fo' = Fo / [(Fv/Fm) + (Fo/Fm')] Requires previous dark-adapted Fv/Fm and Fm' measurements to calculate.	Murchie and Lawson (2013) Maxwell and Johnson (2000) Oxborough and Baker (1997)
Interpretation		Measurement of Fo' using far-red illumination can be open to error if the far-red light does not adequately oxidise Q_A. Additionally, non-photochemical quenching may also relax. Both these factors either individually or combined may result in an overestimation of Fo'. Calculating Fo' in situations where plants are stressed and may experience significant photoinhibition has been queried. However, this is not valid, as the only requirements for the calculation of Fo' to be accurate are: (i) that PSII centres are open at the point of measuring Fo; (ii) that there is no reversal of down-regulation between the measurements of Fo and Fm; and (iii) that there is no reversal of photoinhibition between the measurements of Fm' and Fm. It has been argued that the calculation of Fo' is actually more accurate than the measured value, due to the difficulty in measuring Fo'.	
Fv'	-	Fm' - Fo'	Baker (2008)
Interpretation		Ability of PSII to perform photochemistry (Q_A reduction) in a light-adapted leaf.	
$F_{20\mu s}'$	-	Recorded by FMS-300 at fixed time points during saturating pulses applied to a light-adapted sample. They are thus the logical equivalents of the dark-adapted $F_{20\mu s}$, F_L, F_K, F_J and F_I parameters but for light-adapted samples. Presented as additional data describing the light-adapted response to a saturating pulse and for comparison with the established parameters for dark-adapted induction kinetics. Do not appear to have been discussed in the literature to date.	
F_L'	$F_{100\mu s}'$		
F_K'	$F_{300\mu s}'$		
F_J'	F_{2ms}'		
F_I'	F_{30ms}'		

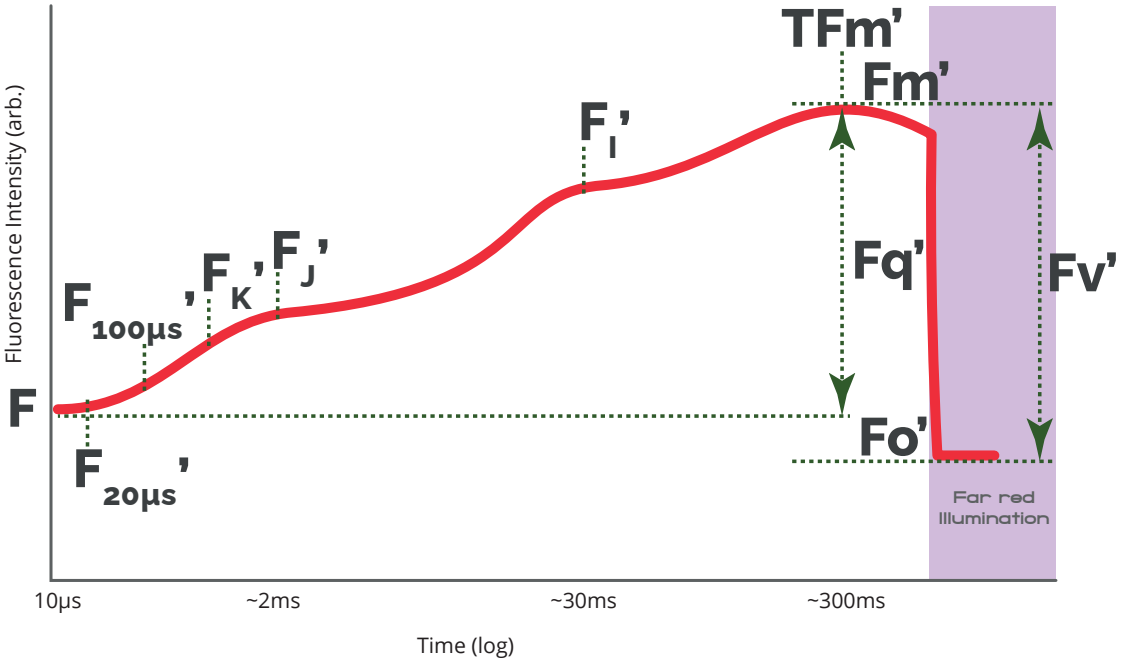

Figure 10. Graph to show where on the fast fluorescence measurement the kinetic parameters are measured.

2.5.2 Parameters: Fast fluorescence ratios

2.5.2.1. The ΦPSII parameter

ΦPSII (also known by the synonyms Fq'/Fm', ΔF/Fm' and Y[II]) is a highly popular parameter, in part due to ease of measurement (no sample dark-adaptation is required) but mainly due to its establishment as an accurate indicator of operational PSII efficiency in the light (Murchie & Lawson, 2013). ΦPSII also correlates closely with linear electron transport, and subsequently, the quantum yield of CO_2 assimilation (Baker, 2008).

In many cases, ΦPSII is a more stress-sensitive parameter than Fv/Fm since it provides a real-time measurement of the effective (current) photosynthetic efficiency of PSII under the prevailing environmental conditions. Factors such as light availability, temperature, and other stress-induced changes in the photosynthetic apparatus can all affect ΦPSII values.

Fv/Fm measures the maximum quantum yield of PSII and is a sensitive indicator of the integrity of PSII reaction centres. It provides information about the maximum potential efficiency of PSII under optimal conditions. While Fv/Fm can indicate stress or damage to PSII when significantly reduced, it may not always detect subtle changes in photosynthetic efficiency caused by environmental stressors. By contrast, ΦPSII is often more sensitive to early stress responses. Stress-induced changes in the photosynthetic apparatus, such as alterations in electron transport rates or energy dissipation mechanisms, can affect ΦPSII before they lead to visible damage detectable by Fv/Fm.

ΦPSII is a dynamic parameter that responds rapidly to changes in environmental conditions, such as fluctuations in light intensity or temperature. It reflects the real-time balance between absorbed light energy used for photosynthesis and energy dissipation mechanisms. It can be used as a measure of the effects of photoinhibition where excessive light leads to damage and reduced efficiency of PSII. Photoinhibition typically results in a decrease in ΦPSII as the efficiency of PSII photochemistry declines. Damage to PSII reaction centres reduces efficiency, leading to a reduction in PSII electron transport.

A change in ΦPSII values can also be measured due to activity of NPQ mechanisms, which dissipate excess absorbed light energy as heat to protect the photosynthetic apparatus. While NPQ helps mitigate photoinhibition, it can also reduce ΦPSII by diverting energy away from linear electron transport. The impact of photoinhibition on ΦPSII may vary depending on the severity and duration of the stress, as well as the plant's ability to repair damaged PSII. Temporary decreases in ΦPSII may occur during periods of photoinhibition, followed by gradual recovery as PSII repair mechanisms restore functionality.

2.5.2.2. Why measure ΦPSII?

The measurement of the ΦPSII parameter can be useful in many different applications. Examples of some of the different experimental applications are as follows:

- **Assessment of photosynthetic efficiency**
  ΦPSII is an indicator of the efficiency of Photosystem II, which is responsible for the initial steps of photosynthesis. By measuring ΦPSII, users can assess how effectively light energy is being converted into chemical energy through the photosynthetic process.
- **Monitoring stress responses**
  Changes in ΦPSII can indicate stress in plants. Environmental factors like drought, excessive light, high temperatures, or nutrient deficiencies can negatively impact ΦPSII. Monitoring ΦPSII allows researchers and plant physiologists to detect and quantify stress responses and potentially take corrective actions.
- **Diagnosing plant health**
  In agricultural and horticultural contexts, measuring ΦPSII can help diagnose the health of plants. Reduced ΦPSII can be an early indicator of plant stress or disease, allowing for early intervention to mitigate damage.

- **Optimizing crop production**
  By monitoring ΦPSII, researchers can optimise growing conditions for crops and maximise their photosynthetic efficiency. This can lead to increased crop yields and more sustainable agricultural practices.
- **Evaluating the effects of genetic modifications**
  ΦPSII measurements can be used to assess the effects of genetic modifications or breeding techniques on the photosynthetic efficiency of plants. This is important for developing crop varieties with improved photosynthetic performance.
- **Studying plant responses to environmental changes**
  Researchers use ΦPSII measurements in studies related to climate change, as it helps in understanding how plants respond to changing environmental conditions, such as increased CO_2 levels or altered temperature patterns.
- **Scientific research**
  ΦPSII measurements provide essential data for scientific research in plant physiology and photosynthesis, helping to better understand the fundamental processes that underlie plant growth and development.
- **Education and outreach**
  ΦPSII measurements are used in educational settings to teach students about photosynthesis and plant biology. They provide a hands-on way to engage students in the study of plant physiology.

The following parameters should be measured on a light-adapted sample.

Parameter	Synonyms	Calculation	References
ΦPSII	Fq'/Fm' ΔF/Fm' Y(II)	(Fm' - F) / Fm'	Genty et al. (1989) Baker (2008) Maxwell and Johnson (2000)
Interpretation		PSII operating efficiency. Estimates the efficiency at which light absorbed by PSII is used for Q_A reduction. At a given photosynthetically active photon flux density (PPFD) this parameter provides an estimate of the quantum yield of linear electron flux through PSII.	
Fv'/Fm'	-	(Fm' - Fo') / Fm'	Baker (2008)
Interpretation		An estimate of the maximum efficiency of PSII photochemistry at a given PPFD. The PSII operating efficiency if all the PSII centres were 'open' (Q_A oxidized).	
V_J'	-	$(F_J' - F) / (Fm' - F)$	-
Interpretation		Represents the relative variable fluorescence at 2 ms (which in a dark- adapted sample would be the J-step of the OJIP curve). This does not appear to have been discussed in the literature to date. Speculatively, the interpretation of V_J' as an estimation of the fraction of reduced Q_A may still be valid although further research would be needed to understand the contribution of reoxidised Q_A, given that the sample is in a light-adapted state. There may be merit in analysing this parameter in relation to qL, which provides an estimation of open PSII RCs.	
V_I'	-	$(F_I' - F) / (Fm' - F)$	-
Interpretation		Relative variable fluorescence at 30 ms (which in a dark-adapted sample would be the I-step of the OJIP curve). As with V_J' above, there may be merit in analysing this parameter with qL.	

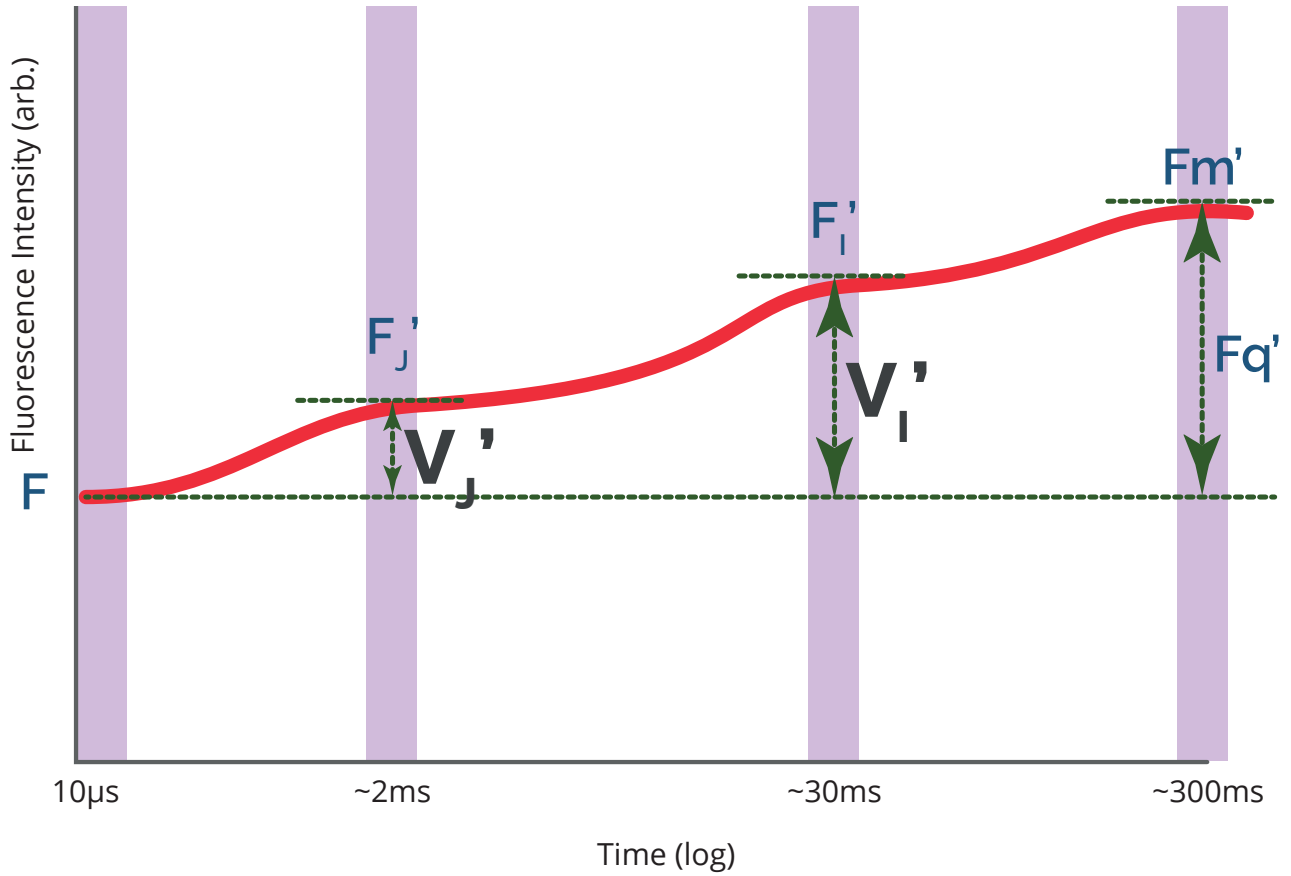

Figure 11. Graph to show where values used in the calculation of ratio parameters are taken from light-adapted fast fluorescence measurements.

3. Quenching analysis

3.1 NPQ mechanisms and components

Non-photochemical quenching (NPQ) is a process in which excess absorbed light energy is dissipated into heat (Ruban 2016). When exposed to high light conditions, PSII reaction centres are rapidly closed which leads to a reduction in the amount of absorbed energy that can be quenched through both photosynthetic and chlorophyll fluorescence pathways. This subsequently leads to a build-up of harmful excitation energy within the photosynthetic membranes which has the potential to damage the PSII reaction centre itself (Ruban 2016).

Whilst mechanisms exist to repair photo-damaged PSII reaction centres, these processes are slow. Sustained pressure from high light can also damage the antenna pigments themselves (Flemming et al 2012) which can then lead to a decline in overall photosynthetic efficiency, and in some cases, death of the photosynthetic cell, tissue or organism (Ruban 2016).

When conducting experiments of non-photochemical quenching, it is important to note that the parameters relating to NPQ are measurements of changes in heat dissipation relative to the dark-adapted state. The same increase in heat dissipation will be characterised by a smaller increase in quenching in situations where the dark-adapted Fm is a higher value. This means that direct comparisons between leaves with different histories or leaves of different species can be ambiguous. In general terms, direct comparison of NPQ from samples with different Fv/Fm should be avoided (Maxwell and Johnson 2000).

NPQ involves several mechanisms and components:

- **Pigment molecules**
  The first step in NPQ is the excitation of chlorophyll and other pigment molecules by absorbed light energy. When the energy level in these pigments exceeds the capacity for photosynthesis, the excess energy needs to be safely dissipated.
- **Xanthophyll cycle**
  A significant part of NPQ involves the xanthophyll cycle, a series of enzymatic reactions that alter the composition of pigments in the thylakoid membranes. The key xanthophyll pigments involved are violaxanthin, antheraxanthin, and zeaxanthin. When light intensity increases, violaxanthin can be converted into zeaxanthin, which has a higher capacity for dissipating excess energy as heat.
- **Proton gradient**
  High light intensity also causes the accumulation of protons (H+) in the thylakoid lumen. This proton gradient is created by the splitting of water during the light-dependent reactions of photosynthesis and is used to drive the production of ATP.
- **PsbS protein**
  The PsbS protein (Photosystem II Subunit S) plays a crucial role in NPQ. In response to excess light, PsbS senses the low pH environment in the thylakoid lumen and triggers the activation of NPQ. It helps to regulate the xanthophyll cycle by activating enzymes that convert violaxanthin to zeaxanthin.
- **Zeaxanthin formation**
  Zeaxanthin formation is a critical step in NPQ. Zeaxanthin is believed to enhance the dissipative capacity of the thylakoid membranes, increasing the conversion of excess energy into heat.
- **Antenna quenching**
  Excess light energy causes a reconfiguration of the light-harvesting antenna complexes associated with PSII. This reconfiguration helps redirect the absorbed energy away from the reaction centres of PSII, reducing the probability of photodamage.
- **Energy dissipation**
  Once zeaxanthin is formed and the antenna complexes are reconfigured, excess energy is dissipated as heat, reducing the energy reaching the reaction centres and protecting the photosynthetic apparatus from photodamage.

For further reading, a detailed review of NPQ can be found in Ruban 2016, “Nonphotochemical Chlorophyll Fluorescence Quenching: Mechanism and Effectiveness in Protecting Plants from Photodamage”, Plant Physiology, Volume 170, Issue 4, April 2016, Pages 1903–1916.

3.2 The typical quenching analysis

FMS-300 offers a routine for the measurements of non-photochemical quenching mechanisms based on the widely cited and reproduced protocol published in Baker & Rosenqvist, 2004, “Applications of chlorophyll fluorescence can improve crop production strategies: an examination of future possibilities”. The purpose of this protocol is to allow investigation of both photochemical and non-photochemical components of chlorophyll fluorescence by measuring under both dark- and light-adapted states.

When configuring the settings for the quenching analysis routine, consideration must be given to the different components of the protocol and how the settings chosen might affect the outcome of the experiment.

For example, in Nies et al., 2021, the authors discussed the time point at which the actinic illumination should be switched on following the initial dark-adapted measurement of Fv/Fm. They observed that in published protocols, they encountered descriptions of settings that were ambiguous and unhelpful when setting up their own experiments. They conducted experiments with a range of different settings.

They found that there were significant effects in lowering the initial NPQ measurement with longer time intervals between the dark-adapted saturating pulse and the onset of actinic illumination. They proposed that a precise knowledge of the NPQ parameter and mechanisms is required for rigorous interpretation of NPQ induction kinetics (Nies et al., 2021).

Figure 12 below shows an example of a quenching analysis protocol. This example is designed to show where specific parameters are derived from within the framework of this analysis protocol. A typical quenching analysis experiment would have more saturating pulse events in both the actinic and dark relaxation phases of the protocol.

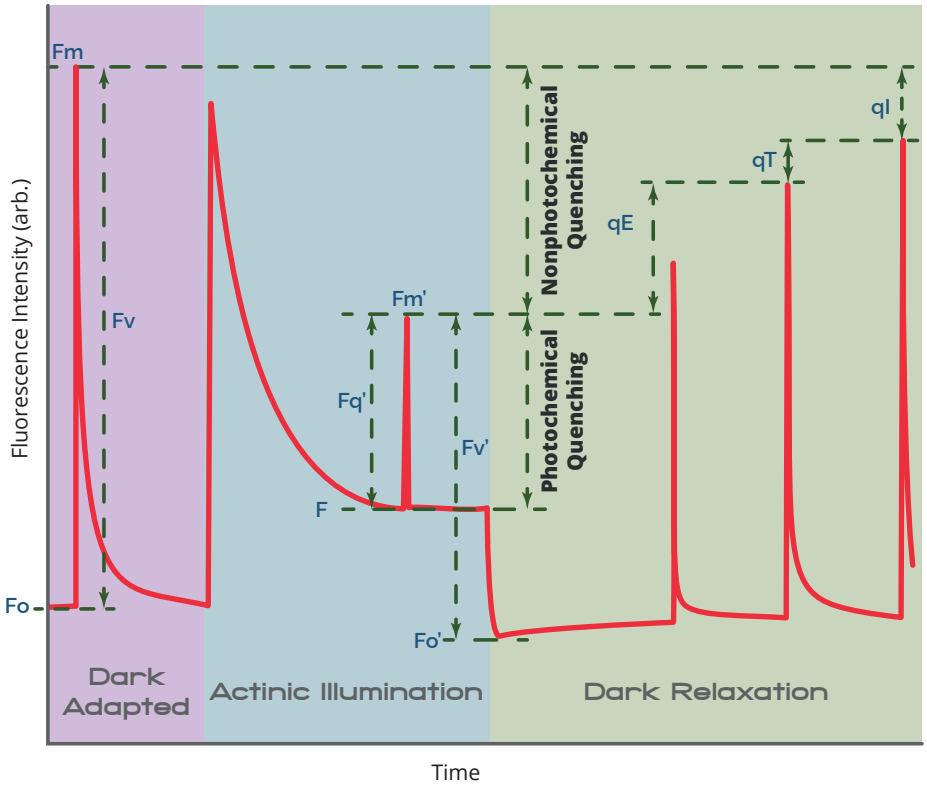

Figure 12. A simplified representation of the Quenching analysis routine used by FMS-300. This figure is modified from the well-known quenching protocol in Baker et al. (2004). It shows where the specific parameters derived during a quenching experiment originate. A typical quenching protocol would consist of more pulses during both the actinic and dark relaxation phases of the protocol.

3.3 Different analysis models for NPQ

Several models have been proposed for the analysis of NPQ.

- Puddle model
  The Puddle model parameters describe a photosynthetic unit (PSU - a complex of pigments and proteins coupled to a reaction centre where the initial light-driven charge separation of photosynthetic reactions takes place. Mauzerall et al., 1989) where each PSII RC is linked to its own antenna system (Kramer et al., 2004).
- Lake model
  The Lake model represents a more realistic model of a PSU where PSII RCs are connected by shared antenna systems (Kramer et al., 2004).
- Simplified Lake model
  The simplified Lake model, proposed by Hendrickson et al., 2004, allows a more straight-forward measurement protocol to measure NPQ without needing to make a measurement of dark-adapted Fo or a measured/calculated Fo'.

3.4 Why measure non-photochemical quenching?

The quenching analysis protocol can provide significant detail about the underlying mechanisms in the light-dependent reactions of photosynthesis. Quenching, as a term, refers to the dissipation of the energy absorbed by the antenna pigments which can consist of 3 different pathways:

1. Photochemical quenching (i.e. photochemistry).
2. Non-photochemical quenching (i.e. thermal dissipation).
3. Chlorophyll fluorescence.

These processes are mutually competitive, so an increase/decrease in one process will result in inverse changes in the other two.

Measuring non-photochemical quenching (NPQ) is an important tool in the study of many different fundamental areas of research including:

- **Photoprotection**
  NPQ is a crucial photoprotective mechanism in photosynthetic organisms. It helps dissipate excess light energy absorbed by antenna pigments, thereby preventing damage to the photosynthetic apparatus. By measuring NPQ, it is possible to assess the capacity of plants to protect themselves from photodamage under high light conditions, which is particularly important for plants growing in environments with fluctuating light intensities or under stress conditions.
- **Stress response**
  NPQ levels can serve as indicators of both biotic and abiotic stress. Environmental factors such as high light, drought, salinity, and extreme temperatures can induce NPQ as a protective response. Monitoring NPQ allows analysis of the impact of various stressors on plant physiology and to identify stress-tolerant genotypes or cultivars for breeding programs or agricultural practices.
- **Photosynthetic efficiency**
  NPQ affects the overall efficiency of photosynthesis by regulating the flow of excitation energy within the photosynthetic machinery. High levels of NPQ can reduce the efficiency of light harvesting and energy conversion processes, leading to decreased photosynthetic rates. Measuring NPQ provides insights into the balance between light absorption and utilisation in photosynthetic organisms, helping to understand the factors that limit photosynthetic efficiency under different environmental conditions.
- **Environmental monitoring**
  NPQ measurements contribute to the understanding of the responses of photosynthetic organisms to environmental changes. By monitoring NPQ levels in field settings or controlled environments, researchers can assess the resilience of plant populations to factors such as climate change, pollution, and habitat degradation. This information is crucial for predicting the impact of environmental stressors on ecosystems and for developing strategies to mitigate their effects.
- **Biological research**
  NPQ measurements provide valuable information for basic research in plant physiology and photosynthesis. Understanding the molecular mechanisms underlying NPQ regulation can lead to insights into the dynamics of energy transfer and dissipation in photosynthetic membranes. This knowledge not only deepens understanding of fundamental biological processes but also informs the development of biotechnological applications aimed at improving crop productivity and stress tolerance.

3.5 Non-photochemical quenching parameters

3.5.1 Parameters: Puddle model for NPQ analysis

This protocol should be executed on a dark-adapted leaf since the calculation requires the dark-adapted Fo and Fm values.

Parameter	Synonyms	Calculation	References
NPQ	-	(Fm – Fm') / Fm' or Fm / Fm' - 1	Kramer et al (2004) Murchie and Lawson (2013) Baker (2008) Muller et al (2001) Ruban et al (2012) Schreiber (2004)
Interpretation		Coefficient of NPQ (Stern-Volmer approach). Light-induced photoprotection through thermal dissipation of energy. Used to infer activity of the Xanthophyll Cycle as it is more sensitive to energy dissipation within the antennae matrix which contain xanthophylls, where energy dependent quenching occurs. A more robust assessment of NPQ than the qN parameter, since it is not dependent upon Fo' and is not affected by Fo quenching.	
qN	-	1 - Fv' / Fv	Ruban (2016)
Interpretation		Used to calculate non-photochemical quenching. This parameter describes the percentage of quenching in a similar manner to ΦPSII.	
qP	-	Fq' / Fv'	Kramer et al (2004) Murchie and Lawson (2013)
Interpretation		Photochemical quenching: relates PSII maximum efficiency to operating efficiency. Non-linearly relates to the proportion of PSII centres in open states based on a puddle model for the photosynthetic unit.	

3.5.2 Parameters: Lake model for NPQ analysis

This protocol should be executed on a dark-adapted leaf since the calculation requires the dark-adapted Fo and Fm values.

Parameter	Synonyms	Calculation	References
ΦPSII	Fq'/Fm' ΔF/Fm' Y(II)	(Fm' - F) / Fm'	Genty et al. (1989) Baker (2008) Maxwell and Johnson (2000)
Interpretation		PSII operating efficiency. Estimates the efficiency at which light absorbed by PSII is used for Q_A reduction. At a given photosynthetically active photon flux density (PPFD) this parameter provides an estimate of the quantum yield of linear electron flux through PSII.	
Y(NPQ)	ΦNPQ	(F / Fm') - (F / Fm)	Kramer et al (2004) Hendrickson et al (2004) Klughammer & Schreiber (2008)
Interpretation		Quantum yield of regulated non-photochemical thermal energy dissipation via ΔpH- and xanthophyll pathways. Competitive pathway with ΦPSII and Y(NO) i.e. Y(NPQ) + Y(NO) + ΦPSII = 1	

Parameter	Synonyms	Calculation	References
Y(NO)	Φ(f,D) Φ(NO)	F/Fm	Kramer et al (2004) Hendrickson et al (2004) Klughammer & Schreiber (2008) Lazar (2016)
Interpretation		Quantum yield of primarily constitutive losses, corresponding to the sum of non-regulated heat dissipation and fluorescence emission. Reflects non-light induced (basal or dark) quenching processes. Competitive pathway with ΦPSII and Y(NPQ) i.e. Y(NPQ) + Y(NO) + ΦPSII = 1	
qL	-	(Fq' / Fv') x (Fo' / F)	Kramer et al (2004) Baker (2008) Murchie and Lawson (2013)
Interpretation		Estimates the fraction of open PSII RCs based on a Stern–Volmer approach using a "lake" or "connected units" model which describes photosynthetic consisting of multiple RCs connected by shared antenna.	

3.5.3 Parameters: Simplified Lake model for NPQ analysis

This protocol should be executed on a dark-adapted leaf since the calculation requires the dark-adapted Fm values.

Parameter	Synonyms	Calculation	References
ΦPSII	Fq'/Fm' ΔF/Fm' Y(II)	(Fm' - F) / Fm'	Genty et al. (1989) Baker (2008) Maxwell and Johnson (2000)
Interpretation		PSII operating efficiency. Estimates the efficiency at which light absorbed by PSII is used for Q_A reduction. At a given photosynthetically active photon flux density (PPFD) this parameter provides an estimate of the quantum yield of linear electron flux through PSII.	
Y(NPQ)	ΦNPQ	(F / Fm') - (F / Fm)	Kramer et al (2004) Hendrickson et al (2004) Klughammer & Schreiber (2008)
Interpretation		Quantum yield of regulated non-photochemical thermal energy dissipation via ΔpH- and xanthophyll pathways. Competitive pathway with ΦPSII and Y(NO) i.e. Y(NPQ) + Y(NO) + ΦPSII = 1	
NPQ	-	(Fm – Fm') / Fm' or Fm / Fm' - 1	Kramer et al (2004) Murchie and Lawson (2013) Baker (2008) Muller et al (2001) Ruban et al (2012) Schreiber (2004)
Interpretation		Coefficient of NPQ (Stern-Volmer approach). Light-induced photoprotection through thermal dissipation of energy. Used to infer activity of the Xanthophyll Cycle as it is more sensitive to energy dissipation within the antennae matrix which contain xanthophylls, where energy dependent quenching occurs. A more robust assessment of NPQ than the qN parameter, since it is not dependent upon Fo' and is not affected by Fo quenching.	

Parameter	Synonyms	Calculation	References
Y(NO)	Φ(f,D) Φ(NO)	F/Fm	Kramer et al (2004) Hendrickson et al (2004) Klughammer & Schreiber (2008) Lazar (2016)
Interpretation		Quantum yield of primarily constitutive losses, corresponding to the sum of non-regulated heat dissipation and fluorescence emission. Reflects non-light induced (basal or dark) quenching processes. Competitive pathway with ΦPSII and Y(NPQ) i.e. Y(NPQ) + Y(NO) + ΦPSII = 1	

4. Light response curves

4.1 Rapid light curves vs. steady-state light curves

The Light Response Curve protocols allow researchers to analyse the electron transport rate (ETR) parameter for periods of actinic illumination with increasing intensity. At the end of the experiment, ETR for each of the actinic light steps can be plotted against PPFD (also know as photosynthetically active radiation - PAR). An algorithm can then be used to calculate parameters including maximum ETR (ETRmax) and the minimum saturating irradiance (Ek).

There are 2 different techniques for the measurement of light response curves using either a steady-state light curve (SSLC) method or the rapid light curve (RLC) technique.

SSLC were used traditionally because they are analogous to more traditional photosynthesis-light response curves (PE) based on C isotope incorporation or oxygen evolution (Houliez et al 2017). SSLC methodology defines periods, or steps, of actinic illumination at a range of intensities with each step duration sufficient to allow steady-state photosynthetic rates to be achieved. There are several disadvantages of this method of measuring light response.

- Measurement of the photosynthetic activity during each light step is influenced, not only by the illumination of the current step, but also by all the steps preceding i.e. the recent light history of the sample.
- Execution of SSLC protocols can take several hours. This is not a convenient method since at reduces capacity for repetition.
- The long duration of SSLC experiments makes it unsuitable for field-based experiments. Significant challenges are presented when comparing results between different plants, as varying factors such as time of day, associated diurnal changes of the plant and dynamic weather conditions must be considered (Rascher et al 2000).
- In addition, in field applications, measuring for long periods of time means that there is huge scope for error due to rapidly fluctuating environmental conditions that could occur during the course of the experiment.

Rapid Light Curves (RLCs) can be used to provide detailed information relating to the saturation characteristics of electron transport through photosystem II (PSII) in addition to overall photosynthetic performance (Ralph & Gademann 2005).

RLCs consist of a series of relatively short (<30s, typically 10s) light steps, with the light intensity increasing at each step. Each light step is interspersed by a saturating pulse where the ETR value is calculated. Unlike the PE light response curves or the SSLC, RLC protocols do not achieve steady-state photosynthetic rates during the light steps. In contrast to PE curves, which provide an indication of optimal state of photosynthetic performance independent of light history, RLCs indicate the current state of photosynthetic performance. Because steady-state conditions are not reached in RLCs, they reflect the light-acclimation state in the period leading up to the measurement and also longer-term light history (Ralph & Gademann 2005).

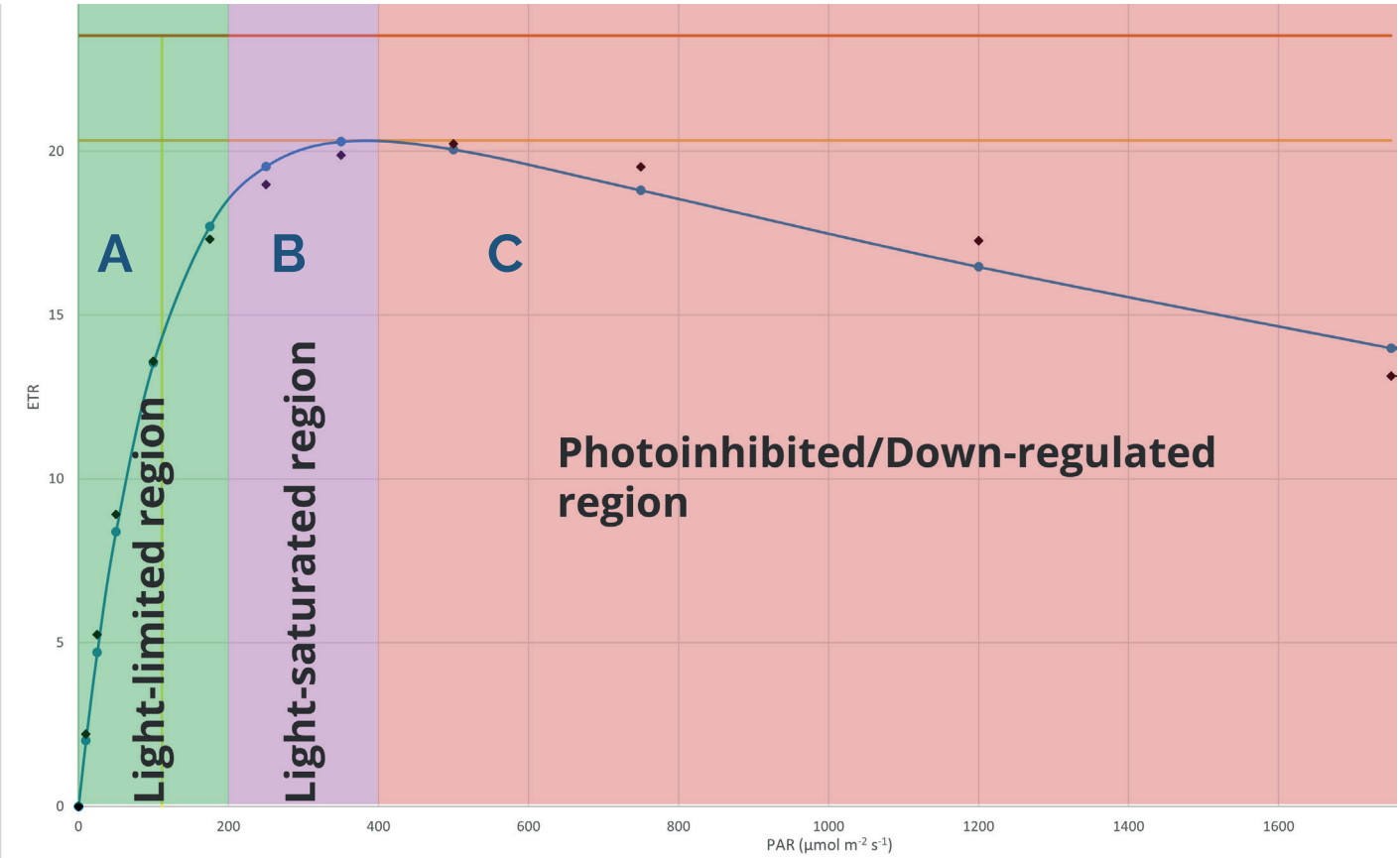

Figure 13. With ETR plotted against PPFD, the graph shows three distinct regions; (A) Light-limited region, (B) Light-saturated region and (C) Photoinhibited/Down-regulated region.

With ETR plotted against PPFD, RLCs show three distinct regions (Figure 13):

- **Light-limited region**
  Photosynthetic rates are limited by low light levels in the light-limited region. The parameter α indicates the slope of the rise of ETR vs. PPFD and is proportional to efficiency of light capture (effective quantum yield or ΦPSII) (Schreiber, 2004).
- **Light-saturated region**
  During this phase, the capacity of the electron transport chain limits the electron transport rate. The ETR vs. PPFD curve reaches a plateau where maximum ETR occurs (denoted by the parameter ETRmax) (Schreiber, 2004). The minimum saturating irradiance, denoted by the parameter Ek (sometimes referred to as Ik), is determined by finding the intercept of α and ETRmax (Sakshaug et al., 1997) and can be related to quenching. Below Ek , photochemical quenching is the dominant pathway whereas non-photochemical quenching is dominant above Ek (Henley, 1993).
- **Photoinhibited/Down-regulated region**
  In this region, where the plant is subjected to supra-saturating light intensities, the ETR vs. PPFD curve often tends to decline, which could be associated with photoinhibition (Henley, 1993). This effect would be more likely to occur with traditional PE or SSLCs, where steady-state photosynthetic rates are achieved. However, as steady-state is not achieved in RLC protocols, there isn't normally sufficient time for photodamage to occur. It has been suggested that the decline of ETR at supra-saturating light intensities could be linked to dynamic down-regulation of PSII (White and Critchley, 1999).

4.2 The ETR parameter

Electron transport rate (ETR), is calculated from a saturating pulse at the end of each actinic light step in a light response curve from the ΦPSII parameter.

In principle, the linear relationship between PSII operating efficiency (ΦPSII) and linear electron flux allows the use of ΦPSII to estimate the noncyclic ETR through PSII (Baker 2008). ETR is calculated as follows:

$$ETR = \Phi PSII \times PAR \times PFDa \times fraction_{PSII}$$

PFDa refers to the amount of incident light received at the leaf surface which is in turn, absorbed by the antenna pigments. This value is frequently assumed to be 0.84, i.e., 84% of incident light. This assumption may be reasonable for many mature green leaves (Baker 2008), but is not always the case and large deviations from this value can frequently occur (Ehleringer 1991, Hodanova 1985, Jones 1992). Caution must be used when comparing samples that are likely to have differing light absorption properties.

Murchie & Lawson (2013), suggested that comparing ETR values in a drought-stressed leaf with a low turgor value with a control hydrated leaf is not appropriate. They continued that leaf samples with different pigment contents or photosystem stoichiometry such as those that have undergone changes in light acclimation state (Anderson et al., 1995) may also suffer inaccuracies.

To achieve the most accurate estimation of ETR, PFDa should be measured using an integrating sphere with a light source similar to that used to drive photosynthesis and a spectroradiometer or quantum sensor (Baker 2008). The resulting value can then be used in the ETR calculation.

As with PFDa described above, the value for $fraction_{PSII}$ is frequently an assumed value, which is 0.5 (Baker 2008). This value represents the proportion of absorbed incident light intercepted by PSII antennae with respect to PSI antennae (Murchie and Lawson 2013). Although the 0.5 value for $fraction_{PSII}$ has been estimated for leaves, it is unlikely to be accurate in many situations (Baker 2008). The procedure required for a more accurate determination of PFDa is not straightforward and involves numerous assumptions (Laisk et al 1996, Laisk et al 2006, Miyake et al 2004). Another problem is that leaves of many species accumulate non-photosynthetic pigments, such as anthocyanins, which can markedly modify not only PFDa but also $fraction_{PSII}$. This is often the case when leaves experience environmental stresses during development (Baker 2008). All things considered, the actual proportionality of light use by each of the photosystems is extremely difficult to quantify accurately, and therefore, the use of the 0.5 assumed value is frequently used (Murchie and Lawson 2013) in the absence of a known value.

4.2.1 Curve fitting algorithm

A light response curve protocol generates values of ETR for a set of given PAR (also know as photosynthetically active photon flux density - PPFD) intensities. From this data, a curve that models the relationship between PAR and ETR can be calculated. The plotted curve is a line of best fit for the measured data. For the FMS-300 instrument, the line of best fit is modelled using the Levenberg-Marquardt algorithm (Levenberg, 1944 and Marquardt, 1963) which was developed to solve non-linear least squares problems.

The algorithm finds values for the parameters α, β and ETRs for a curve with the best fit to the measured data. It then repeats the calculation, fine-tuning the values of the parameters until it reaches a stable solution to the equation with the least error. These parameter values can be used in the equation to plot a curve and to calculate values of ETR_{max} and E_k.

The value calculated for α is the slope of the linear part of the curve, the light-limited region at low PAR values. β is the slope at the end of the curve (at higher PAR values). ETRs is the maximum possible ETR if there is no decrease in ETR at higher PAR levels. ETR_{max} is the maximum ETR value of the curve. E_k is the minimum saturating irradiance, the PAR value corresponding to the point at which the extrapolated linear part of the curve (where α is determined) reaches ETR_{max}.

4.3 Light Response Curve parameters

4.3.1 Parameters: Light response curves

If measuring a rapid light curve, the literature suggests that a short period of dark-adaptation should be used prior to the first saturating pulse (Schreiber 2004, Rascher et al., 2000). For steady-state light response curves where the kinetics of NPQ are also of interest, a fully dark-adapted sample should be used for the protocol.

Parameter	Synonyms	Calculation	References
ETR	J	PAR x PFD_a x $fraction_{PSII}$ x ΦPSII	Murchie and Lawson (2013) Baker (2008)
Interpretation		Non-cyclic electron transport rate through PSII	
JNPQ	-	Y(NPQ) x PFD_a x $fraction_{PSII}$	Hendrickson et al (2004)
Interpretation		The rate of energy dissipation via ΔpH and xanthophyll-regulated thermal dissipation	
PAR	PPFD		
Interpretation		Ambient PAR values from the PTL-100 leafclip or user-defined PAR values from routine settings.	
α	-	Levenberg–Marquardt algorithm	Schreiber (2004) Gavin (2019)
Interpretation		Indicates the slope of the rise of ETR vs. PPFD and is proportional to efficiency of light capture (effective quantum yield or ΦPSII).	
β	-	Levenberg–Marquardt algorithm	Henley (1993) White and Critchley (1999) Gavin (2019)
Interpretation		Where the plant is subjected to supra-saturating light intensities, the ETR vs. PPFD curve often tends to decline, which could be associated with photoinhibition. This effect would be more likely to occur with traditional P – E or steady state light curves, where steady-state photosynthetic rates are achieved. However, as steady-state is not achieved in RLC protocols, there isn't normally sufficient time for photodamage to occur. It has been suggested that the decline of ETR at supra-saturating light intensities could be linked to dynamic down-regulation of PSII.	
ETR_{max}	-	Levenberg–Marquardt algorithm	Schreiber (2004) Gavin (2019)
Interpretation		During the light-saturated phase of a rapid light curve, the capacity of the electron transport chain limits the electron transport rate. When ETR vs. PPFD is plotted, the curve reaches a plateau where maximum ETR occurs.	
E_k	I_k	Levenberg–Marquardt algorithm. The PAR value from the horizontal axis where the intercept between α and ETR_{max} occurs.	Sakshaug et al (1997) Henley (1993) Gavin (2019)
Interpretation		The minimum saturating irradiance for electron transport through PSII. Can be related to quenching. Below E_k, photochemical quenching is the dominant pathway whereas non-photochemical quenching is dominant above E_k.	

5. References

1. Anderson JM, Chow WS, Park YI. 1995. The grand design of photosynthesis: acclimation of the photosynthetic apparatus to environmental cues. Photosynthesis Research 46, 129–139.
2. Neil R. Baker, Eva Rosenqvist, Applications of chlorophyll fluorescence can improve crop production strategies: an examination of future possibilities, Journal of Experimental Botany, Volume 55, Issue 403, August 2004, Pages 1607–1621, https://doi.org/10.1093/jxb/erh196
3. Baker NR. Chlorophyll fluorescence: a probe of photosynthesis in vivo. Annu Rev Plant Biol. 2008;59:89-113. doi: 10.1146/annurev.arplant.59.032607.092759. PMID: 18444897.
4. Banks JM.
   Continuous excitation chlorophyll fluorescence parameters: a review for practitioners.
   Tree Physiol. 2017 Aug 1;37(8):1128-1136.
5. Barboričová, M., Filaček, A., Vysoká, D. M., Gašparovič, K., Živčák, M., & Brestic, M.
   Sensitivity of fast chlorophyll fluorescence parameters to combined heat and drought stress in wheat genotypes.
   Plant, Soil and Environment, 68(7), 309-316. (2022).
6. Bednaříková, M., Folgar-Cameán, Y., Kučerová, Z., Lazár, D., Špundová, M., Hájek, J., & Barták, M.
   Special issue in honour of Prof. Reto J. Strasser – Analysis of K- and L-band appearance in OJIPs in Antarctic lichens in low and high temperature.
   Photosynthetica, 58(SPECIAL ISSUE), 646-656 (2020).
7. Shiguo Chen, Juan Yang, Mansong Zhang, Reto Jörg Strasser, Sheng Qiang, Classification and characteristics of heat tolerance in Ageratina adenophora populations using fast chlorophyll a fluorescence rise O-J-I-P, Environmental and Experimental Botany, Volume 122, 2016, Pages 126-140, ISSN 0098-8472, https://doi.org/10.1016/j.envexpbot.2015.09.011. (https://www.sciencedirect.com/science/article/pii/S0098847215300216)
8. Cuchiara, C. C., Silva, I. M. C., Martinazzo, E. G., Braga, E. J. B., Bacarin, M. A., & Peters, J. A.
   Chlorophyll fluorescence transient analysis in Alternanthera tenella Colla plants grown in nutrient solution with different concentrations of copper.
   Journal of Agricultural Science, 5(8), 8. (2013).
9. David Dewez, Vasilij Goltsev, Hazem M. Kalaji, Abdallah Oukarroum,
   Inhibitory effects of silver nanoparticles on photosystem II performance in Lemna gibba probed by chlorophyll fluorescence,
   Current Plant Biology, Volume 16, December 2018
10. Demmig B, Björkman O. 1987. Photon yield of O2 evolution and chlorophyll fluorescence characteristics at 77 K among vascular plants of diverse origins. Planta 170, 489–504.
11. Demmig-Adams B, William W. Adams I. 2006. Photoprotection in an ecological context: the remarkable complexity of thermal energy dissipation. New Phytologist 172, 11–21.
12. Ehleringer JR. 1991. Temperature and energy budgets. In Plant Physiological Ecology, ed. RWPearcy, J Ehleringer, HA Mooney, PWRundel, pp. 97–135. London: Chapman and Hall
13. Fleming, Graham R., et al. “Design principles of photosynthetic light-harvesting.” Faraday discussions 155 (2012): 27-41.

14. Force, L., Critchley, C. & van Rensen, J.J. New fluorescence parameters for monitoring photosynthesis in plants. Photosynthesis Research 78, 17–33 (2003). https://doi.org/10.1023/A:1026012116709

15. Gavin, Henri P.
"The Levenberg-Marquardt algorithm for nonlinear least squares curve-fitting problems."
Department of civil and environmental engineering, Duke University 19 (2019).

16. Bernard Genty, Jean-Marie Briantais, Neil R. Baker,
The relationship between the quantum yield of photosynthetic electron transport and quenching of chlorophyll fluorescence,
Biochimica et Biophysica Acta (BBA) - General Subjects, Volume 990, Issue 1, January 1989

17. Gliozeris, S., Tamosiunas, A. and Stuopyte, L.
Effect of Some Growth Regulators on Chlorophyll Fluorescence in Viola x wittrockiana "Wesel Ice".
Biologija, 53, 24-27 (2007)

18. Gonzalez-Mendoza, D., Espadas y Gil, F., Santamaría, J. M., & Zapata-Perez, O.
Multiple effects of cadmium on the photosynthetic apparatus of Avicennia germinans L. as probed by OJIP chlorophyll fluorescence measurements.
Zeitschrift Für Naturforschung C, 62(3-4), 265-272. (2007).

19. Govindjee and Rajni Govindjee
Photosynthesis and the "Z"-scheme
University of Illinois at Urbana-Champaign
E-mail: gov@uiuc.edu
URL: http://www.life.uiuc.edu/govindjee

20. Hassannejad, S.; Lotfi, R.; Ghafarbi, S.P.; Oukarroum, A.; Abbasi, A.; Kalaji, H.M.; Rastogi,
A. Early Identification of Herbicide Modes of Action by the Use of Chlorophyll Fluorescence Measurements.
Plants 2020, 9, 529.

21. Hendrickson, L., Furbank, R.T. & Chow, W.S. A Simple Alternative Approach to Assessing the Fate of Absorbed Light Energy Using Chlorophyll Fluorescence. Photosynthesis Research 82, 73–81 (2004).

22. Henley WJ (1993). Measurement and interpretation of photosynthetic light-response curves in algae in the context of photoinhibition and diel changes. J Phycol 29:729–738

23. Hill R and Bendall F (1960). Function of two cytochrome components in chloroplasts: a working hypothesis. Nature 186:136–140

24. Hodanova D. 1985. Leaf optical properties. In Photosynthesis during Leaf Development, ed. Z Sestak, pp. 107–127. Praha: Academia

25. Houliez, E., Lefebvre, S., Lizon, F., Schmitt, F.G., (2017). Rapid light curves (RLC) or non-sequential steady-state light curves (N-SSLC): which fluorescence-based light response curve methodology robustly characterizes phytoplankton photosynthetic activity and acclimation status? Mar Biol (2017) 164:175

26. Jones HG. 1992. Plants and Microclimate (2nd edition). Cambridge: Cambridge Univ. Press. 428 pp.

27. Kalaji, M.H., Goltsev, V.N., Żuk-Gołaszewska, K., Zivcak, M., & Brestic, M.
Chlorophyll Fluorescence: Understanding Crop Performance — Basics and Applications (1st ed.).
CRC Press. (2017).

28. Kalaji, H.M., Jajoo, A., Oukarroum, A. et al.
Chlorophyll a fluorescence as a tool to monitor physiological status of plants under abiotic stress conditions.
Acta Physiol Plant 38, 102 (2016).

29. Kalaji, H.M., Schansker, G., Brestic, M. et al.
Frequently asked questions about chlorophyll fluorescence, the sequel.
Photosynth Res 132, 13–66 (2017).

30. Kautsky, H. and A. Hirsch (1931). Chlorophyllfluoreszenz und Kohlensäureassimilation. Naturwissenschaften, 19, 964

31. Kramer, D.M., Johnson, G., Kiirats, O. et al.
New Fluorescence Parameters for the Determination of QA Redox State and Excitation Energy Fluxes.
Photosynthesis Research 79, 209–218 (2004).

32. Klughammer, Christof, and Ulrich Schreiber.
"Complementary PS II quantum yields calculated from simple fluorescence parameters measured by PAM fluorometry and the Saturation Pulse method."
PAM application notes 1.2 (2008): 201-247.

33. Hendrik Küpper, Zuzana Benedikty, Filis Morina, Elisa Andresen, Archana Mishra, Martin Trtílek, Analysis of OJIP Chlorophyll Fluorescence Kinetics and QA Reoxidation Kinetics by Direct Fast Imaging, Plant Physiology, Volume 179, Issue 2, February 2019, Pages 369–381, https://doi.org/10.1104/pp.18.00953

34. Laisk A, Loreto F. 1996. Determining photosynthetic parameters from leaf CO2 exchange and chlorophyll fluorescence. Ribulose-1,5-bisphosphate carboxylase/oxygenase specificity factor, dark respiration in the light, excitation distribution between photosystems, alternative electron transport rate, and mesophyll diffusion resistance. Plant Physiol. 110:903–12

35. Laisk A, Eichelmann H, Oja V, Rasulov B, R¨amma H. 2006. Photosystem II cycle and alternative electron flow in leaves. Plant Cell Physiol. 47:972–83

36. Lazár, Dusan. The polyphasic chlorophyll a fluorescence rise measured under high intensity of exciting light. Functional Plant Biology. 33. 9-30. 10.1071/FP05095. (2006).

37. Lazár, Dusan. A Word Or Two About Chlorophyll Fluorescence And Its Relation To Photosynthesis Research. A text for Ph.D. students. (2016). 10.13140/RG.2.1.4243.0329.

38. Lazár D, Jablonský J
On the approaches applied in formulation of a kinetic model of photosystem II: different approaches lead to different simulations of the chlorophyll a fluorescence transients.
J Theor Biol 257(2):260–269 (2009)

39. Levenberg, Kenneth (1944). "A Method for the Solution of Certain Non-Linear Problems in Least Squares".
Quarterly of Applied Mathematics. 2 (2): 164–168. doi:10.1090/qam/10666.

40. Rong-hua LI, Pei-guo GUO, Baum Michael, Grando Stefania, Ceccarelli Salvatore,
Evaluation of Chlorophyll Content and Fluorescence Parameters as Indicators of Drought Tolerance in Barley,
Agricultural Sciences in China, Volume 5, Issue 10, October 2006

41. Marquardt, Donald (1963). "An Algorithm for Least-Squares Estimation of Nonlinear Parameters". SIAM Journal on Applied Mathematics. 11 (2): 431–441. doi:10.1137/0111030. hdl:10338.dmlcz/104299.

42. Kate Maxwell , Giles N. Johnson, Chlorophyll fluorescence—a practical guide, Journal of Experimental Botany, Volume 51, Issue 345, April 2000, Pages 659–668, https://doi.org/10.1093/jexbot/51.345.659

43. Masojídek, J.; Ranglová, K.; Lakatos, G.E.; Silva Benavides, A.M.; Torzillo, G. (2021). Variables Governing Photosynthesis and Growth in Microalgae Mass Cultures. Processes, 9, 820.

44. David Mauzerall, Nancy L. Greenbaum, The absolute size of a photosynthetic unit, Biochimica et Biophysica Acta (BBA) - Bioenergetics, Volume 974, Issue 2, 1989, Pages 119-140, ISSN 0005-2728, https://doi.org/10.1016/S0005-2728(89)80365-2.

45. Miyake C, Shinzaki Y, Miyata M, Tomizawa K. 2004. Enhancement of cyclic electron flow around PSI at high light and its contribution to the induction of nonphotochemical quenching of chl fluorescence in intact leaves of tobacco plants. Plant Cell Physiol. 45:1426–33

46. Morin P (1964) Études des cinétiques de fluorescence de la chlorophylle in vivo, dans les premiers instants qui suivent le début de l'illumination. J Chem Phys 61:674–680

47. Patricia Müller, Xiao-Ping Li, and Krishna K. Niyogi.
"Non-Photochemical Quenching. A Response to Excess Light Energy."
Plant Physiology 125, no. 4 (2001): 1558–66.

48. E.H. Murchie , T. Lawson, Chlorophyll fluorescence analysis: a guide to good practice and understanding some new applications, Journal of Experimental Botany, Volume 64, Issue 13, October

49. Neubauer, Christian and Schreiber, Ulrich. "The Polyphasic Rise of Chlorophyll Fluorescence upon Onset of Strong Continuous Illumination: I. Saturation Characteristics and Partial Control by the Photosystem II Acceptor Side" Zeitschrift für Naturforschung C, vol. 42, no. 11-12, 1987, pp. 1246-1254. https://doi.org/10.1515/znc-1987-11-1217

50. Nies, Tim & Niu, Yuxi & Ebenhöh, Oliver & Matsubara, Shizue & Matuszyńska, Anna. (2021). Chlorophyll fluorescence: How the quality of information about PAM instrument parameters may affect our research. https://doi.org/10.1101/2021.05.12.443801.

51. Oxborough K, Baker NR.
Resolving chlorophyll a fluorescence images of photosynthetic efficiency into photochemical and non-photochemical components—calculation of qP and Fv'/Fm' without measuring Fo'.
Photosynthesis Research 54, 135–142. 1997.

52. Platt, T., Gallegos, C.L., Harrison, W.G. (1980). Photoinhibition of photosynthesis in natural assemblages of marine phytoplankton. J. Mar. Res., 38: 687-401

53. Ralph, P.J. & Gademann, R. (2005). Rapid light curves: a powerful tool to assess photosynthetic capacity. Aquat. Bot., 82: 222–237.

54. L. van Rensburg, G.H.J. Krüger, P. Eggenberg, R.J. Strasser,
Can screening criteria for drought resistance in Nicotiana tabacum L. be derived from the polyphasic rise of the chlorophyll a fluorescence transient (OJIP)?,
South African Journal of Botany, Volume 62, Issue 6, December 1996

55. Rascher, U., Liebig, M., Lüttge, U., (2000). Evaluation of instant light-response curves of chlorophyll fluorescence parameters obtained with a portable chlorophyll fluorometer on site in the field. Plant Cell Environ. 23, 1397–1405.

56. Rohácek K, Barták M
Technique of the modulated chlorophyll fluorescence: basic concepts, useful parameters, and some applications. Photosynthetica 37:339–363. (1999)

57. Rosenqvist, E. and Van Kooten, O.
Chlorophyll Fluorescence: A General Description and Nomenclature.
In: DeEll, J.R. and Toivonen, P.M.A., Eds., Practical Applications of Chlorophyll Fluorescence in Plant Biology, Kluwer Academic Publishers, 31-37 (2003).

58. Alexander V. Ruban, Nonphotochemical Chlorophyll Fluorescence Quenching: Mechanism and Effectiveness in Protecting Plants from Photodamage, Plant Physiology, Volume 170, Issue 4, April 2016, Pages 1903–1916, https://doi.org/10.1104/pp.15.01935

59. Ruban AV, Johnson MP, Duffy CD.
The photoprotective molecular switch in the photosystem II antenna.
Biochim Biophys Acta. 2012 Jan;1817(1):167-81.

60. Sakshaug, E., Bricaud, A., Dandonneau, Y., Falkowski, P.G., Kiefer, D.A., Legendre, L., Morel, A., Parslow, J., Takahshi, M., (1997) Parameters of photosynthesis: definitions, theory and interpretation of results. J Plankton Res 19:1637–1670

61. Samborska-Skutnik, I.A. & Kalaji, Hazem & Sieczko, Leszek & Bąba, Wojciech.
Structural and functional response of photosynthetic apparatus of radish plants to iron deficiency.
Photosynthetica. 58. 10.32615/ps.2019.132. (2019).

62. Schreiber, U.
Pulse-Amplitude-Modulation (PAM) Fluorometry and Saturation Pulse Method: An Overview.
In: Papageorgiou, G.C., Govindjee (eds) Chlorophyll a Fluorescence. Advances in Photosynthesis and Respiration, vol 19. Springer, Dordrecht. https://doi.org/10.1007/978-1-4020-3218-9_11 (2004).

63. Srivastava, A. & Strasser, Reto.
Constructive and destructive action of light on the photosynthetic apparatus.
Journal of Scientific and Industrial Research. 56. 133-148. (1997).

64. Srivastava A, Strasser RJ, Govindjee
Greening of peas: parallel measurements of 77 K emission spectra, OJIP chlorophyll a fluorescence transient, period four oscillation of the initial fluorescence level, delayed light emission, and P700.
Photosynthetica 37:365–392 (1999)

65. Stirbet A, Govindjee.
On the relation between the Kautsky effect (chlorophyll a fluorescence induction) and Photosystem II: basics and applications of the OJIP fluorescence transient.
J Photochem Photobiol B. 2011 Jul-Aug;104(1-2):236-57.

66. Stirbet, A., Govindjee Chlorophyll a fluorescence induction: a personal perspective of the thermal phase, the J–I–P rise. Photosynth Res 113, 15–61 (2012). https://doi.org/10.1007/s11120-012-9754-5

67. Stirbet, A., Riznichenko, G.Y., Rubin, A.B. et al. Modeling chlorophyll a fluorescence transient: Relation to photosynthesis. Biochemistry Moscow 79, 291–323 (2014). https://doi.org/10.1134/S0006297914040014

68. Strasser RJ, Strasser BJ (1995) Measuring fast fluorescence transients to address environmental questions: the JIP test. In 'Photosynthesis: from light to biosphere.Vol. V'. (Ed. P Mathis) pp. 977–980. (Kluwer Academic Publishers: Dordrecht)

69. Strasser RJ, Srivastava A, Tsimilli-Michael M The fluorescence transient as a tool to characterize and screen photosynthetic samples. In: Mohanty P, Yunus, Pathre (eds) Probing photosynthesis: mechanism, regulation and adaptation. Taylor and Francis, London, pp 443–480 (2000)

70. Strasser, R.J., Tsimilli-Michael, M. and Srivastava, A.
Analysis of the Chlorophyll a Fluorescence Transient.
In: Papageorgiou, G.C. and Govindjee, Eds., Chlorophyll a Fluorescence: A Signature of Photosynthesis, Springer, New York, 321-362 (2004).

71. Strasser RJ, Govindjee
On the O–J–I–P fluorescence transient in leaves and D1 mutants of Chlamydomonas reinhardtii.
In 'Researching photosynthesis. Vol. 2'. (Ed. M Murata) pp. 29–32. (KluwerAcademic Publishers: Dordrecht) (1992)

72. Tomek P, Lazár D, Ilık P, Naus J (2001) On the intermediate steps between the O and P steps in chlorophyll a fluorescence rise measured at different intensities of exciting light. Australian Journal of Plant Physiology 28, 1151–1160.

73. Tsimilli-Michael M.
Revisiting JIP-test: An educative review on concepts, assumptions, approximations, definitions and terminology.
Photosynthetica. 2020 Jan 1;58(special issue):275-92.

74. Tsimilli-Michael M., Strasser R.J.:
In vivo assessment of stress impact on plants' vitality: applications in detecting and evaluating the beneficial role of mycorrhization on host plants.
In: Varma A. (ed.): Mycorrhiza. State of the Art, Genetics and Molecular Biology, Eco-Function, Biotechnology, Eco-Physiology, Structure and Systematics. 3rd edition. Pp. 679-703. Springer, Berlin-Heidelberg 2008

75. White, A.J., & Critchley, C. (1999). Rapid light curves: a new fluorescence method to assess the state of the photosynthetic apparatus. Photosynth. Res., 59, 63–72.